AD_____

Award Number: W81XWH-08-1-0376

TITLE: **Pathological Fingerprints, Systems Biology and Biomarkers of Blast Brain Injury**

PRINCIPAL INVESTIGATOR: **Stanislav Svetlov, MD, PhD**

CONTRACTING ORGANIZATION:

Banyan Biomarkers, Inc.
Alachua, FL 32615

REPORT DATE: **June 2010**

TYPE OF REPORT: **Annual**

PREPARED FOR: **U.S. Army Medical Research and Materiel Command**
Fort Detrick, Maryland 21702-5012

DISTRIBUTION STATEMENT:

X Approved for public release; distribution unlimited

REPORT DOCUMENTATION PAGE

Form Approved
OMB No. 0704-0188

1. REPORT DATE *(DD-MM-YYYY)*	2. REPORT TYPE	3. DATES COVERED *(From - To)*
06/14/2010	Annual	15 MAY 2009-14 MAY 2010

4. TITLE AND SUBTITLE

Pathological Fingerprints, Systems Biology and Biomarkers of Blast Brain Injury

5a. CONTRACT NUMBER

5b. GRANT NUMBER
W81XWH-08-1-0376

5c. PROGRAM ELEMENT NUMBER

6. AUTHOR(S)
PI: Stanislav Svetlov, MD, PhD

ssvetlov@banyanbio.com

5d. PROJECT NUMBER

5e. TASK NUMBER

5f. WORK UNIT NUMBER

7. PERFORMING ORGANIZATION NAME(S) AND ADDRESS(ES)

Banyan Biomarkers, Inc.

Alachua, FL 32615
USA

8. PERFORMING ORGANIZATION REPORT NUMBER

9. SPONSORING / MONITORING AGENCY NAME(S) AND ADDRESS(ES)
U.S. Army Medical Research and Materiel Command
Fort Detrick, Maryland 21702-5012

10. SPONSOR/MONITOR'S ACRONYM(S)

11. SPONSOR/MONITOR'S REPORT NUMBER(S)

12. DISTRIBUTION / AVAILABILITY STATEMENT

Approved for public release; distribution unlimited

13. SUPPLEMENTARY NOTES

14. ABSTRACT We compared the effects of primary blast OP exposure of controlled duration, peak pressure and transmitted impulse with brain injury by a severe blast load accompanied with strong head acceleration. The off-axis rat positioning avoided strong head acceleration due to blast generator venting gas impulse, and reproduced primary blast with different mechanisms. sICAM, L-selectin and E-selectin accumulated substantially in rat blood 24 h after blast and persisted for 14 days post-blast. Serum matrix metalloproteinases (MMP) exhibited a similar profile. Nerve growth factor beta-NGF in blood was significantly elevated within the first week post-blast showing most pronounced changes when the total animal body was subjected to blast wave. Resistin accumulated in rat blood 7 d after blast followed by a gradual decline. Neuropeptide Orexin A content showed drastic raise at 24 h after blast targeting total body, followed by gradual decline. In contrast, blast wave targeting only animal head caused gradual raise of Orexin through 30 d post exposure. For all biomarkers the detected levels raised at all the setups studied, nevertheless most significant and persistent serum changes were observed when the total animal body was subjected to blast wave compared to setups where only animal head was targeted. Proteomic profiling of novel biomarkers has been performed and results are being analyzed.

15. SUBJECT TERMS
blast peak overpressure; brain injury, CNPase, GFAP, NSE, E-selectin, L-selectin; Resistin; Orexin;NGF-beta

16. SECURITY CLASSIFICATION OF:			17. LIMITATION OF ABSTRACT	18. NUMBER OF PAGES	19a. NAME OF RESPONSIBLE PERSON
a. REPORT	b. ABSTRACT	c. THIS PAGE			19b. TELEPHONE NUMBER *(include area code)*
U	U	U	UU	50	USAMRMC

Standard Form 298 (Rev. 8-98)
Prescribed by ANSI Std. Z39.18

Table of Contents

Introduction.

Existing experimental setups for studies of blast effects in small animals have significant flaws in their design impeding precise modeling of primary blast injury. Here, we compared the effects of primary blast OP exposure of controlled duration, peak pressure and transmitted impulse with brain injury by a severe blast load accompanied with strong head acceleration.

During year 2 of project, we determined critical components of pathological pathways as potential markers of blast responses. Brain-specific markers: GFAP and UCH-L1. Group markers:sICAM, L-selectin, E-selectin, beta-NGF, Fractalkine, Resistin and Orexin were examined via ELISA, antibody microarrays and Western blot following blast exposure of different magnitude and durations. **The objectives** of this portion of project has been examine key molecular signatures of vascular, systemic and neuroinflammatory, and neuron-glial components of blast brain injury using both targeted approach and differential neuroproteomic platforms.

BODY

SOW1. **Refine, characterize and create quantitative index for our existing overpressure wave /shock tube model for rat blast brain injury (Year 1)**

During the first year of the project, we delivered and validated shock tube with highly controlled parameters of blast. We defined a Blast Impact Index (**task1**) as a as a combined function of blast wave magnitude at the body surface (peak overpressure in psi, kPa), duration (ms) and distance from the nozzle. We determined mortality and gross pathology at different rat setups in relation to blast impact and assessed threshold of blast (**task 2**). Neurohistology analyses (silver staining) demonstrated neurodegeneration, predominantly in deeper areas of midbrain (**task 3**).

However, we noticed rat head movement and deformation recorded by high speed video upon this severe head-directed blast wave exposure for 10 msec. Due to the complex nature of the blast event the brain injury is a result of a combined impact of the "composite" blast including all 3 major phases of a shockwave. Gas venting jet, albeit lower in magnitude, lasts the longest, represents the bulk of blast impulse and, possibly produces the most devastating impact.

These points to a significant flaw in several previous studies described in the literature: animal specimens are usually placed along the axis of the shock wave generator. In such location, the venting gas jet creates a much larger impulse (mechanical energy transfer) in the specimen than the pressure shock wave itself. Such effect is an experimental artifact since victims of explosive shock waves would not experience such venting gas jet.

Off-axis exposure models 'pure' Blast Peak Overpressure Exposure. Normal explosions produce blast winds that follow behind the incident shock. This effect is mimicked by shock tubes as the wave spherically expands.

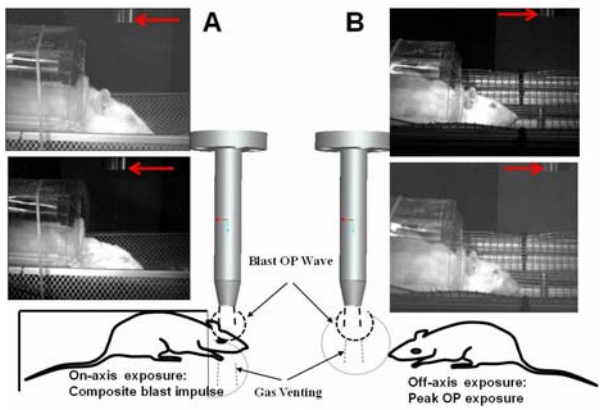

Fig. 1. Different rat positions toward shock tube exit nozzle: on-axis (A) and off-axis (B). Placing rats outside shock tube axis avoids gas venting effect and exposes rat to a peak overpressure: primary blast. Images were taken using high speed camera with ~3,000 frames per second (fps).

Positional characteristics and values of peak OP, duration and impulse were calibrated depending on the angle and distance from nozzle (Fig. 2 A) and tabulated (Fig. 2B

A

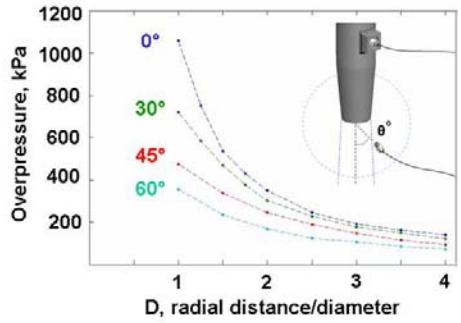

B

	Angle Nozzle/ Head	Distance		Peak Over-pressure (psi/kPa)	Positive Phase Duration (µs)	Impulse/Unit Area (kPa-s)
		D	cm			
	0°	2	5.08	52.6/361	NA	NA
	0°	4	10.16	20.3/140	NA	NA
level 1	30°	2.5	6.35	33.9/234	113.8	10.6
	30°	4	10.16	17.7/122	138.0	8.37
	45°	2	5.08	35.2/243	53.1	6.46
level 2	45°	4	10.16	13.8/95	85.3	4.04
	60°	2	5.08	24.5/169	32.9	2.76
level 3	60°	4	10.16	10.6/73	60.3	2.20

Fig. 2A: Distance from nozzle-peak overpressure curves at different angles of rat head related to nozzle. **2B**: Calculated values of PO, duration and impulse.

In year 1 of the project, we demonstrated up-regulation of GFAP in hippocampus and cortex of rats subjected to severe on-axis blast of 52 psi for 10 msec. During **year 2,** we examined the levels of GFAP in CSF and serum during time-course after 'composite' blast exposure and compared with primary blast.

***SOW2.* Examine key molecular signatures of vascular and neuron-glial components of blast brain injury using both targeted approach and differential neuroproteomic platforms:**

Task4: *Determine molecular components of targeted pathways contributing to acute and subacute blast-induced brain injury*.

Task4(i) Vascular responses and dysregulation of cell adhesion molecules as bridges connecting vascular-endothelial-neural tissue disturbances: E-selectin and L-selectin.

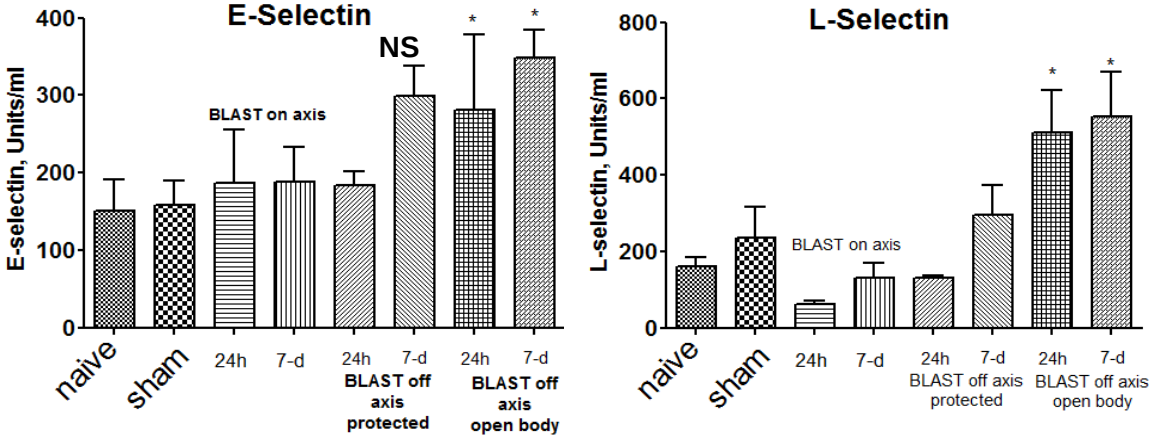

Fig. 3 Levels of L-selectin and E-selectin in serum after different types of blast exposure. Rats were subjected to off-axis head + total body blast: 33.9psi, 113 msec, 10.6 kPa-sec with body armored or uncovered. Blood was collected and cytokines were assayed in serum using RayBiotech L-arrays and expressed in arbitrary Units/ml. Data are Mean+SEM of 3 independent

experiments (rats), each assay performed in triplicate. *=p<0.05 vs. sham (noise exposed rats) according unpaired t-test analysis. NS- Not significant.

E-selectin and L-selectin are adhesion molecules which characterize the activation of vascular component of inflammation and interaction of circulatory cells with endothelial component of blood-brain-barrier (BBB).

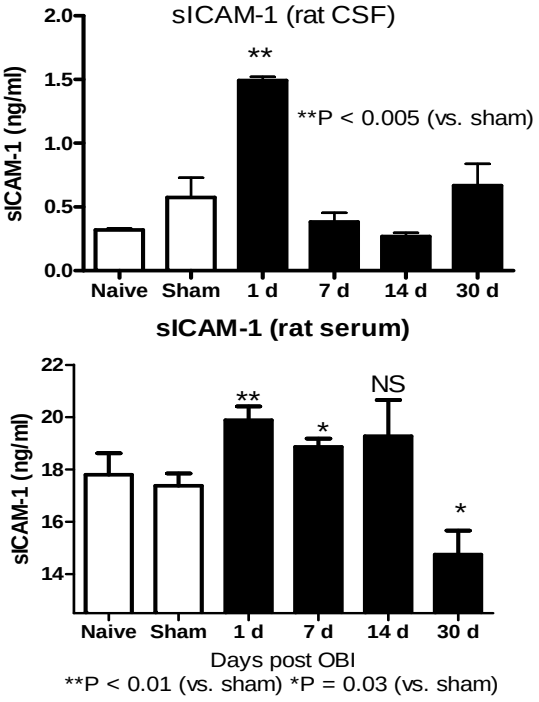

Fig. 4 . Significant accumulation of sICAM in CSF and increase in serum after blast exposure

As can be seen in **Figure 3**, the most prominent activation of vascular components of blast responses occurs when peak overpressure interacts with the frontal part of head without significant acceleration: "flowing blast insight the brain" (blast off-axis open body). Similarly to Selectins, soluble intercellular adhesion molecules play a role in cell-to-cell communications in various vascular responses to stressors,including sheqar stress and blast wave. sICAM was measured in CSF and serum using SW ELISA and significantly accumulated in CSF and serum 24 hours after blast.

Task 4 (ii) Systemic and Neuroinflammmation as further development of impaired vascular reaction in the brain, resulting in enhancement of endothelial permeability/leakage, infiltration of macrophages from circulation and activation of brain-resident microglia cells:

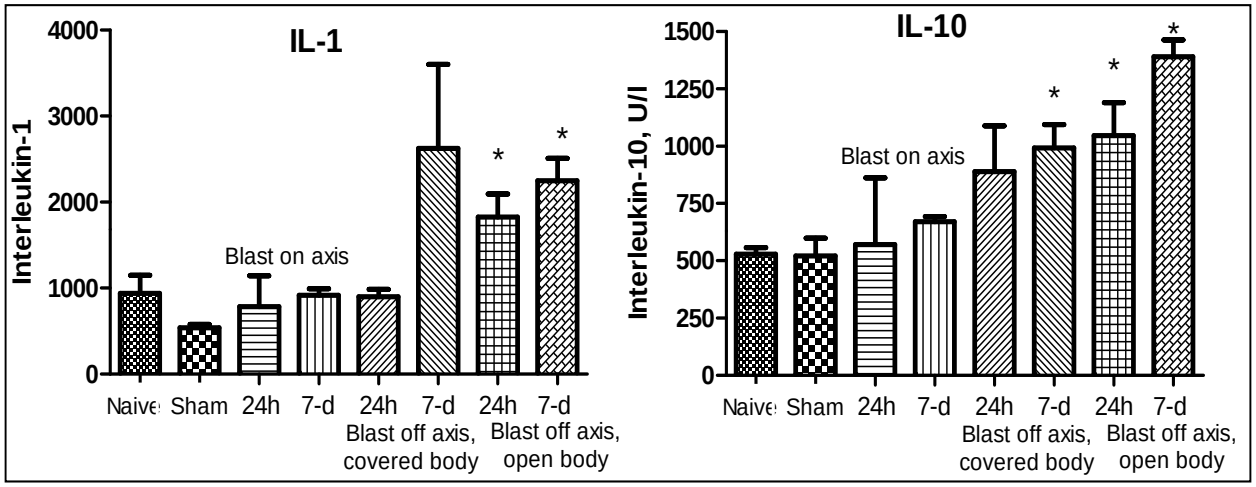

Fig. 5. Serum IL-1 and IL-10 at different times post-blast on- and off-axis.
Note: the most prominent response occurs when OP wave 'flows inside the brain'- off axis frontal exposure with open body. *=p<0.05 vs. naïve/sham was considered as statistically significant according to unpaired t-test, NS-Not significant

As can be seen in Fig. 5, both pro-inflammatory (IL-1) an d counteracting anti-inflammatory molecules (IL-10) accumulate in circulation at 24 hour after open body exposure to frontal (off axis) blast. Moreover, C X3CL1 chemokine Fractalkine was also significantly elevated after different types of b last further suggesting systemic compo nent in response to blast (Fig. 6)

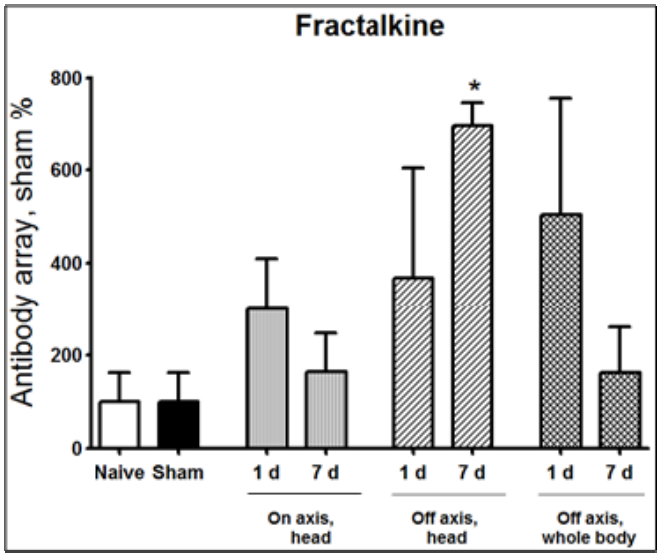

Fig. 6 . Levels of Fractalkine after different types of blast.
*p<0.05, t-test, NS-not significant

Consistent with our hypothesis of transitional **<u>vascular/tissue inflammatory</u>** response to blast, we detected a substantial increase of **matrix metalloproteinases** (MMPs) in serum (Fig. 7).

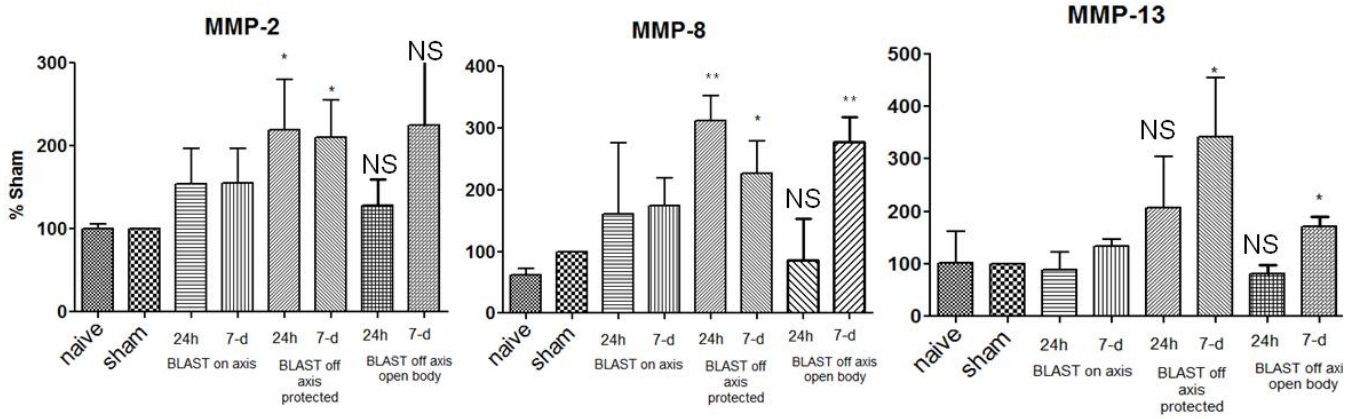

Fig. 7. Serum levels of metalloproteinases after different forms of blast. MMPs were measured using Quantibody arrays (Ray Biotech) and expressed as % of sham values (set as 100 %). Data are Mean<u>+</u>SEM of 3 independent experiments (rats), each assay performed in triplicate. *-p<0.05 and **-p<0.01 using unpaired t-test.

<u>Task 4 (iii)-Neuron-Glia cell damage pathways.</u> We measured CSF and serum levels of GFAP and UCHL-1, biomarkers of glia and neuron activation, respectively, after 'composite blast' exposure and 'peak OP exposure.' We have shown during the first year that GFAP

expression in the hippocampus was increased after composite blast (**Svetlov et al. J. of Trauma, 2010).**

Here, we demonstrate that it has been accompanied by its rapid and statistically significant accumulation in serum 24 h after injury followed by a decline thereafter **(Fig. 8A)**.

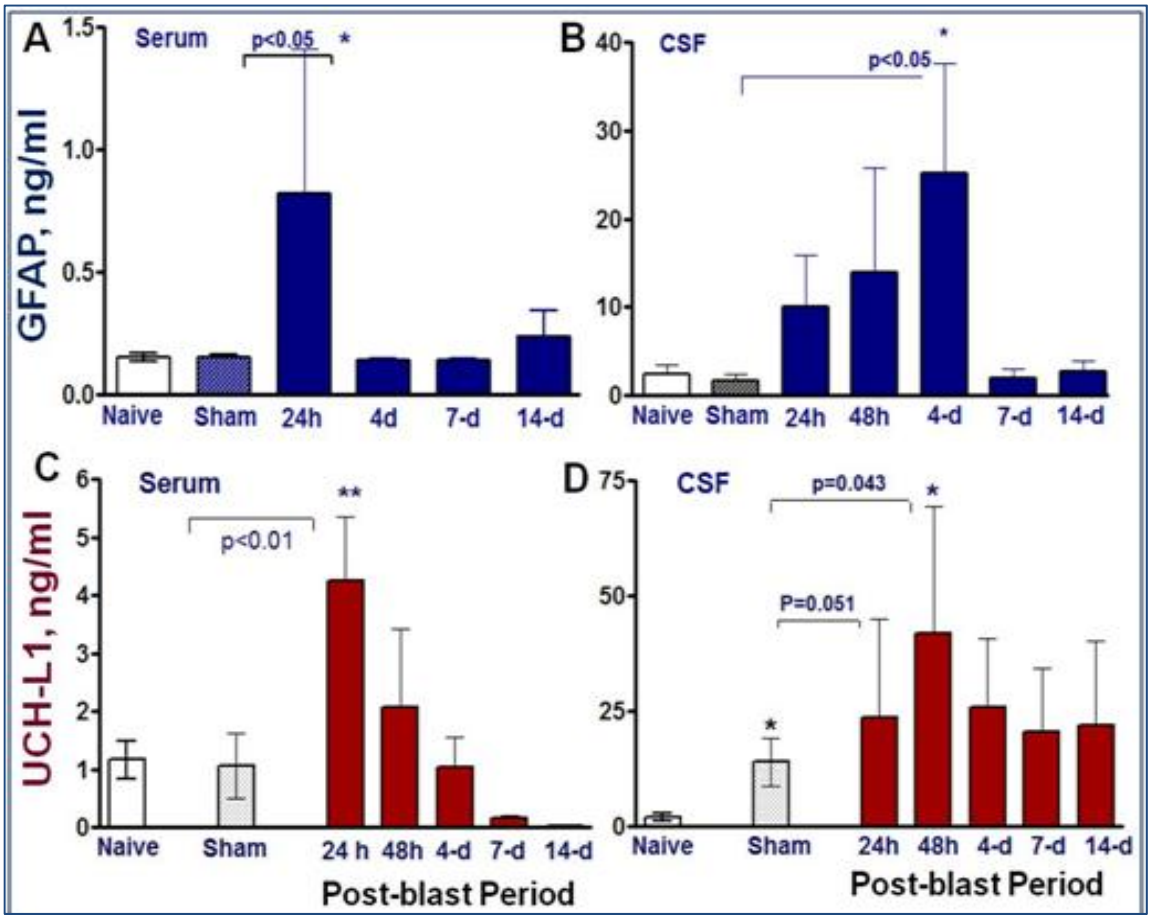

Fig. 8. GFAP content in serum (A) and CSF (B) after blast exposure determined by commercial SW ELISA. Accumulation of UCH-L1 in serum (C) and CSF (D) assayed by Banyan SW ELISA. p values <0.05 shown as statistically significant vs. sham using unpaired t-test

Ubiquitin C-terminal hydrolase-L1 (UCH-L1) has been shown to be a potential biomarker for TBI in CCI models in rats. To assess UCH-L1 concentration in CSF and blood, we developed and employed a proprietary SW ELISA Kit. UCH-L1 rapidly accumulated in the blood 24 hours after blast exposure followed by a gradual decline by 14 days post-blast recovery period **(Fig. 8C).**

Average CSF levels of UCH-L1 were slightly increased throughout the 14 days after blast exposure and, similar to GFAP, varied significantly in individual rats **(Fig. 8D).** These data

suggest an increase of neuronal ubiquitination that may contribute to neurodegeneration as a consequence of blast exposure.

When rats were subjected to blast exposures off-axis the shock tube with a blast wave of moderate magnitude (33.9 psi/234 kPa) hitting the Head+Total body, the increase in serum GFAP was still significant at 48 h **(Fig.9: left panel)** as opposed to direct head exposure, and declined by 4 days post-blast. In contrast, serum UCH-L1 **(Fig.9: right panel)** accumulation was slower and weaker but sustained out to 4 days post-blast, significantly longer than after severe head-directed, body-protected) blast.

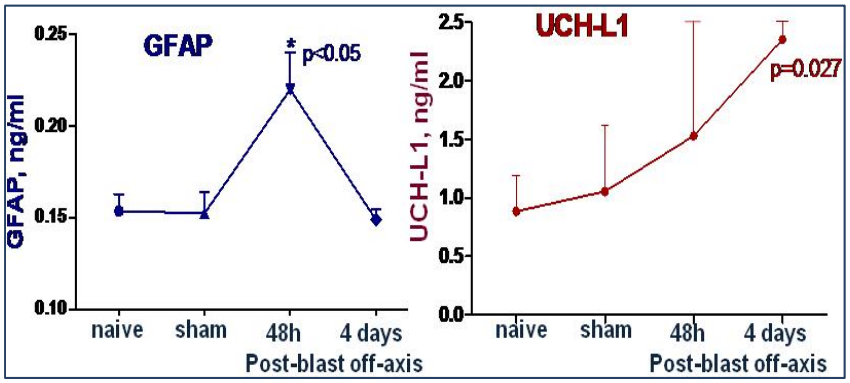

Fig. 9: Serum GFAP and UCH-L1 after off-axis rat exposure to a single blast peak OP of 33.9 psi for 113 µsec; head + body unprotected. Each value represent a Mean+SEM of 3 rat samples fromeach group performed in duplicate. $p<0.05$ (GFAP at 48 h post blast) and $p=0.027$ (UCH-L1, 4 days post blast) were considered statistically significant compared to naïve according unpaired t-test.

Taken together, a characteristic time-course of GFAP and UCH-L1 indicate a potential blood-brain barrier (BBB) disruption after severe blast exposure triggering the pathological events in the brain that lead to hemorrhages, glyosis, glia/neuronal interactions and may lead to neuronal degeneration. Studies are under way to collect more rat samples and improve statistical analysis.

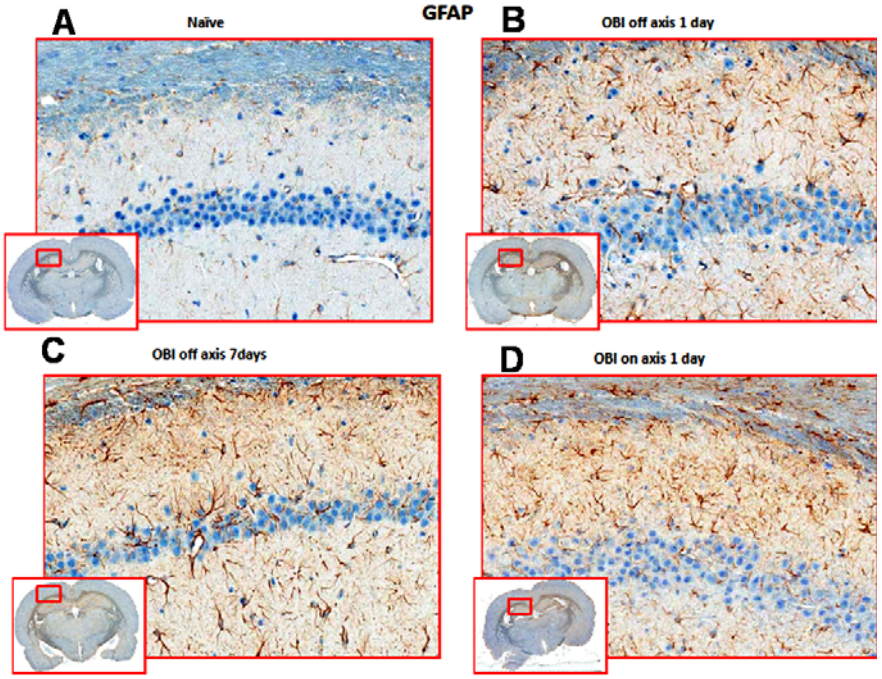

Fig. 10. GFAP immunohistochemistry of hippocampus after different blast exposures. A: sham; B:24 h after off axis blast; C: 7 days after off-axis blast; D: 24 h after on-axis blast. Brain area sections examined are squared in the whole brain images insets. Brown color indicates GFAP positive astrocytes.

To obtain additional evidence of GFAP topical up-regulation in deeper areas of brain, we performed GFAP immunohistochemistry. As can be seen at the Immunohistochemistry panel on previous page, off-axis primary blast exposure results in sustained astroglyosis in hippocampus area (**Fig. 10 B and C,** brown stain) similarly to on-axis brain tissue GFAP upregulation **(Fig. 10D)** which we reported previously.

Task5: **Identify additional biochemical pathways by neuroproteomic approach and integrate the biochemical signatures using System Biology algorithm to construct a blast brain injury network map**

First, we proposed that exposure to blast waves stimulates changes in energy metabolism associated with neuroendocrine responses.

Neuroendocrine components of blast response. Resistin is an adipose tissue peptide, possibly linking insulin resistance/sensitivity and inflammation. Orexin A is a hypothalamic neuropeptide important in CNS regulation of an energy balance, food intake, wakefulness. We measured serum Resistin and Orexin A levels after blast exposure using 2 different methods- Quantibody array (Ray Biotech) and conventional SW ELISA Kits (Bachem). See Figure 11:

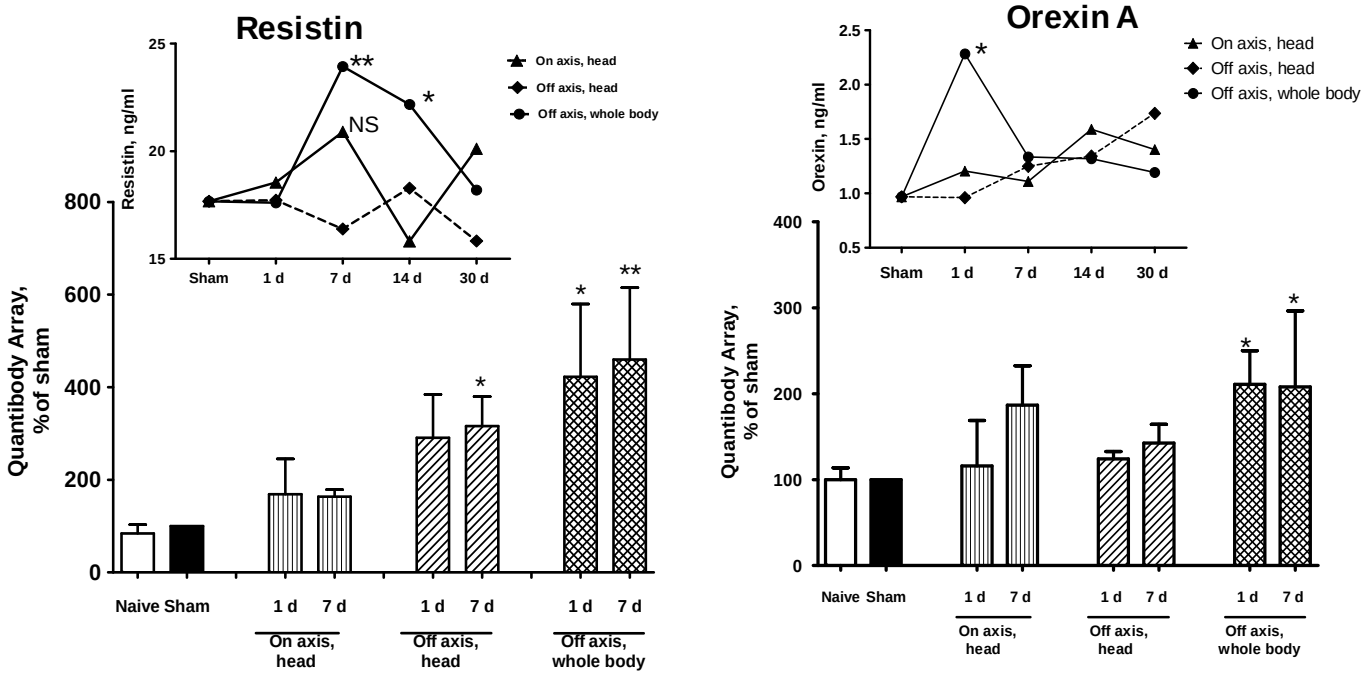

Fig. 11 Time-course of serum Resistin and Orexin A following different types of blast exposure.

Quantibody arrays data are presented as Mean+SEM of 3 independent measurements of at least 3 rats in each group. *-p<0.05, **-p<0.01 vs. sham according unpaired t-test.

Insets in the panels: Resistin and Orexin A levels in serum assayed by EIA Kit (Bachem, Orexin A) or SW ELISA (Resistin, Ray Biotech) and expressed in ng/ml/. Means of 3 independent measurements obtained from at least 2 rats of each group is shown. Unpaired t-test analysis was performed where applicable. Due to a substantial variability of values determined by EIA and ELISA in individual rats, and limited # of samples at time reported, the significance of p values did not match completely to those determined by Quatibody arrays. Additional series of blast experiments and assays of Resistin and Orexin A are under way to improve statistical analyses. However, preliminary conclusions are that, similarly to vascular and neuroinflammation components (interleukins, selectins and MMPs), the increases of Resistin and Orexin are most prominent when blast OP hits the rat through a frontal part without significant cervico-angular acceleration. The specific hypothesis is that blast overpressure results in deregulation of neuroendocrine balance and affects energy metabolism.

Consistent with **task5,** using targeted approach, we identified additional component of neurotrophic response to blast exposure. Serum levels of Nerve Growth Factor beta (beta-NGF) was assessed using SW ELISA after blast exposure at different set-up. The results are presented in **Figure 12** below.

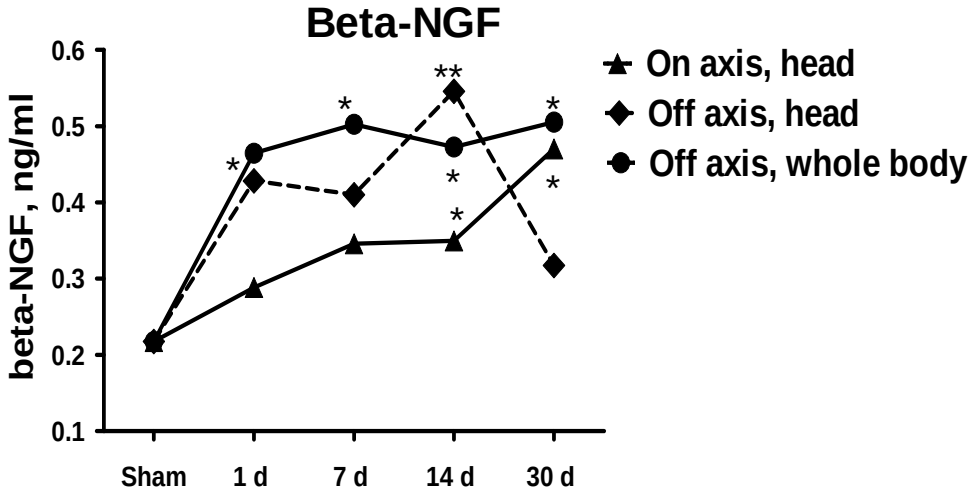

Fig. 12 Time-course of serum beta-NGF following on-axis vs. off axis positions (primary blast overpressure only). Data point represents Mean values of at least 3 rat samples from each group and time points. *-p<0.05 and **-p<0.01 vs. sham group according to unpaired t-test.

Beta-NGF has been suggested to play a neurotrophic role in several neurodegenerative diseases (see Calissano et al. Cell Death Differ. 2010 Jul;17(7):1126-33. for review). Our data indicate that beta-NGF may also have neuroprotective functions and be involved in adaptive responses/neurorepair after blast induced TBI. As can be seen, exposure of whole body to primary overpressure blast instigated a rapid and sustained accumulation of beta-NGF in serum. Detailed analysis of beta-NGF patterns after blast exposures is under way.

Task5: Identify additional biochemical pathways by neuroproteomic approach and integrate the biochemical signatures using System Biology algorithm to construct a blast brain injury network map

We are identifying additional biochemical pathways by neuroproteomic approach and will integrate the biochemical signatures using System Biology algorithm to construct a blast brain injury network map. Proteomic analysis of midbrain tissue at 1 and 7 days after blast has been performed and in process of compared to naïve samples. The raw proteome data of rat midbrain after blast exposure obtained using CAX-PAGE-MS/MS are presented below**.** The creation of network map is under way utilizing PathwayStudio Software.

Global Neuroproteomics OBI Samples Summary

Efforts have been made to perform a global putative biomarker screening for the control vs OBI (1 day and 7 day) study on animal models. Each pooled rat ipsilateral brain tissue from 3 individual, control, 24h and 7d post-OBI, were compared and were processed and resolved by side-by-side multidimensional protein separation. Differential proteins are selected and trypsinized for peptide analysis by RPLC-MSMS. Peptide data is then analyzed by bioinformatic software to identify the differential protein and confirm differential abundance. Differential proteins identification has been finished on OBI samples. Protein separation with dual phase ion-exchange chromatography in tandem with polyacrylamide gel electrophoresis (CAX-PAGE) has already been finished on CCI 24h and 7d post-CCI brain tissue. Twenty one fractions are collected after ion-exchange column. Compared to naïve control brain, each fraction from different control/CCI time points has been run side-by-side on SDS-PAGE gels. Further differential protein identifications and validation are now in the process.

Anion/Cation-Exchange Chromatography

For this aim, we utilized a well-characterized *offline* multidimensional protein separation platform compatible with applying high throughput proteomic technology for biomarker identification. This platform consisted of ion chromatography which is composed of a sulfoproyl –strong cation exchange column (SCX-S1) and a quaternary ammonium- strong anion (SAX-Q1) modified sepharose prepacked ion-exchange columns (Bio-Rad) connected in tandem along with a QuadTec UV detector and BioFrac fraction collector. This platform was termed as cation-anion exchange (CAX) chromatography. For this study, cortex protein samples from each group (control, OBI Day 1, OBI Day 7) of rats (n=5) are pooled to achieve a requisite protein quantity of 1 mg per single injection and to average inconsistent protein levels due to biological variability. CAX Buffers consisted of ice cold 20 mM Tris-HCl (pH 7.5) as buffer A. Elution gradient was performed with 1 M NaCl in 20 mM Tris-HCl as buffer B at a flow rate of 1ml/min. A four-step elution gradient was performed with Buffer B with a linear transition from 0 to 16% B in 7 mL, followed by 16 to 30% B in 9 mL followed by 30 to 40% B in 2 ml and finally 40 to 60% B in 3 ml and then re-equilibrated to 0% B in 4 mL. UV Chromatograms were collected at a wavelength of 280 and 214 nm for each run, see **Fig 1** for differential comparison. Twenty two, 1 ml fractions were collected via the BioFrac fraction collector into 1.5-mL microfuge tubes. Leammli sample buffer (25 µL) was added to the YM-10 collection filters prior to collection by centrifugation at 3500 rpm for 3 min.

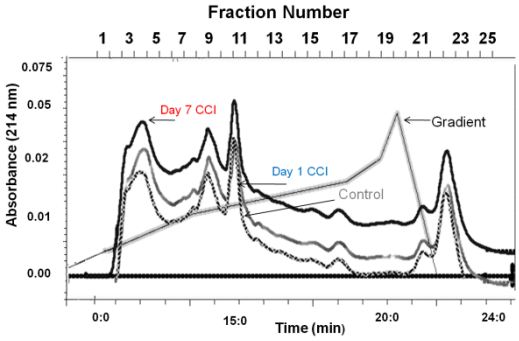

SDS PAGE Analysis

For SDS-1D-PAGE analysis, Control, OBI Day 1, OBI Day 7 protein fractions were run side-by-side (i.e., Control fraction 1 next to fraction 1 Day 1, next to day 7 fraction 1, etc.) using 18-well, 10–20% gradient Tris-HCl Bio-Rad Criterion gels for differential comparison of Control, Day1 CCI and Day 7 CCI samples. NIH ImageJ software (version 1.6, NIH, Bethesda, MD) will be used for

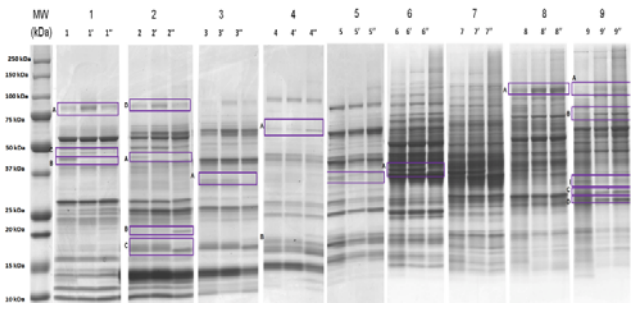

quantitative densitometric analysis of gel band intensity. Any differential expression of 2 or more will be excised for Mass Spec analysis. Differential bands were boxed and labeled according to their 2D position (e.g. the top band excised from the lane of fraction 6 was labeled 6A). In this analysis, 66 fraction were collected [22 fraction from each control, OBI 1Day, OBI 7Day) were collected and run side by side See **Fig 2** for a reperesentative gel of our 1D CAX seperation.

Neuroproteomics Data Analysis :

The Gel Analysis , out of all the 22 fractions collected from each run (control, 1 day, and 7 days), 26 protein bands showed upregulation compared to 11 bands with more than 2 fold downregulation. An average of 4-6 protein were identified from each band these proteins were matched with their exact moelcular weight and compared to the "gel molecular weight". Peptide covarage from mass spectrometry of each identified along moelcular weight criteria were used to consider the proteins as potential hit for validation via western blotting. Among the upregulated proteins identified, a group of metabolic proteins such as phosphoglycerate kinase, Aconitate hydratase and Hexokinase-1. Another set of upregulated proteins constituted break down products such as **Neurofascin (Mwt 137 kDa and identified at 72 kDa) and synaptojanin 1(Mwt 172 kDa and identified at 100 kDa). The whole list of altered proteins (upregulationand down regulation are being organized in two tables).**

NeuroSystems Biology analysis

As to the Neurosystems Biology analysis, we used protein bioinformatics tool "Pathway Architect" by (Ariadne Genomics) to construct and search known protein functions, pathways and protein interactions associated with the differential findings from our neuroproteomics analysis. This analysis was performed at our facilty which has a license to the powerful bio-informatics software Pathway Architect necessary for the neuroproteomic massive data obtained. Analysis was based on the level of trust, interaction direction, effects, mechanisms and tissue specificity. Analysis can be conducted with a choice of 7 algorithms (Analyze networks, analyze transcription regulation, direct interactions, shortest paths, self regulations, expand by one interaction, and auto expand). The importance of such data analysis can not be overstressed; it enables the visualization of biologically relevant networks linking the proteins in specific altered cluster and identify biological processes of each network with statistics and scores. One of the

major aims of these tools include connecting identified biomarkers with patho-physiological information and networks of interest as well as providing **"hypothesis extension"** from the verified proteins to other proteins that may be changing in the clinical samples. Preliminary analysis of the proteomics data identified major pathways -Apoptosis pathway, -Autophagy -Synpatic dysfunction, -Inflammatory pathway -MAP kinase, pathways were among the prominent pathwys altered in CCI-induced brain injury.

Task 5. Proteins up- and down-regulated in midbrain after blast exposure.

	Proteomic Analysis of Blast Injury using CAX-PAGE-MS/MS					
	Protein Name	S_Calculated M	Gel_MW	Number of Unique Peptides		
Gel		(kDa)	(kDa)	Control	Day 1	Day 7
1A	**Aconitate hydratase, mitochondrial**	**85,418.10**	**80 kDa**	**25**	**32**	**24**
1B	**Phosphoglycerate kinase 1**	**44,521.00**	**45 kDa**	**7**	**6**	**3**
1B	Isoform Mitochondrial of Fumarate hydratase, mitoch	54,446.30		6	2	4
1B	Fumarylacetoacetase	45,958.30		3	6	2
1B	Aspartate aminotransferase, mitochondrial	47,297.00		9	6	3
1C	Isoform Mitochondrial of Fumarate hydratase, mitoch	54,446.30	50 kDa	9	11	6
2A	BRO1 domain-containing protein BROX	46,175.80	45 kDa	2	-	-
2A	**Phosphoglycerate kinase 1**	**44,521.00**		**7**	**4**	**5**
2A	Isoform Mitochondrial of Fumarate hydratase, mitoch	54,446.30		3	4	3
2A	Isoform Short of Succinate-semialdehyde dehydroger	52,779.30		9	8	7
2A	Fumarylacetoacetase	45,958.30		5	3	2
2A	Isoform M1 of Pyruvate kinase isozymes M1/M2	57,958.70		13	4	6
2A	Glucose-6-phosphate isomerase	62,811.30		11	-	-
2A	Alpha-enolase	47,111.00		-	-	4
2B	**Glycolipid transfer protein**	**23,686.90**	**22 kDa**			**5**
2B	Glutathione S-transferase Mu 5	26,612.30		?	?	2
2B	**Protein DJ-1**	**19,956.30**				**9**
2B	Peptide methionine sulfoxide reductase	25,832.70				2
2B	Glutathione S-transferase P	23,421.80				3
2C	19 kDa protein	18,561.10	18 kDa	4	3	2
2C	**Protein DJ-1**	**19,956.30**		**4**	**2**	**-**
2C	**Cofilin-1**	**18,515.20**		**3**	**2**	-
2E	Aconitate hydratase, mitochondrial	85,418.10	80 kda	31	42	35
3A	L-lactate dehydrogenase A chain	36,432.80	35 kDa	12	14	8

4A	**Aconitate hydratase, mitochondrial**	**85,418.10**	**65 kDa**	**-**	**??**	**10**
4A	Acyl-CoA synthetase family member 2, mitochondria	67,869.60		3	6	8
4A	Glucose-6-phosphate isomerase	62,811.30		3	7	9
4B	Peptidyl-prolyl cis-trans isomerase A	17,856.80		-	-	2
4B	Adenylate kinase isoenzyme 1	21,566.40		-	-	5
5B	L-lactate dehydrogenase A chain	36,432.80	35 k Da	16	12	5
5B	Ester hydrolase C11orf54 homolog	34,974.80		4		
5B	Thiosulfate sulfurtransferase	33,388.50		10	9	2
5B	Pyridoxal kinase	34,889.20		10	9	5
6A	Malate dehydrogenase, cytoplasmic	36,465.90	37 kDa	6	8	3
6A	Malate dehydrogenase, mitochondrial	35,666.20		5	8	7
6A	calcium binding protein 39	39,857.10		3	6	-
6A	similar to glyceraldehyde-3-phosphate dehydrogenas	35,765.20		12	13	11
8A	**Hexokinase-1**	**102,392.90**	**105 kDa**	**24**	**30**	**30**
8A	ATP citrate lyase isoform 1	120,766.50		7	-	4
8A	Elongation factor 2	95,268.00		5	7	4
8A	Contactin-1	113,479.10		-	2	-
9A	Isoform 4 of Dynamin-1	97,571.50	105 kDa	9	16	18
9A	DnaJ (Hsp40) homolog, subfamily C, member 6	102,171.80		-	5	-
9A	103 kDa protein	102,526.10		-	3	2
9A	Phosphorylase	96,759.10		-	12	6
9A	active BCR-related	97,678.50		-	6	5
9A	Hexokinase-1	102,392.90		-	24	22
9A	99 kDa protein	99,435.90		-	11	9
9A	Elongation factor 2	95,268.00		-	3	-
9A	UDP-N-acetylglucosamine--peptide N-acetylglucosa	116,939.20		-	-	2
9B	**Isoform IA of Synapsin-1**	**73,970.30**	**72 kDa**	**7**	**14**	**15**
9B	**Heat shock cognate 71 kDa protein**	**70,854.70**		**15**	**25**	**26**
9B	Stress-70 protein, mitochondrial	73,840.40		6	10	10
9B	RCG61183, isoform CRA_b	77,860.80		-	3	-
9B	Plastin-3	70,664.50		-	2	6
9B	**Isoform 1 of Neurofascin**	**137,987.60**		**-**	**2**	**3**
9B	Succinate dehydrogenase [ubiquinone] flavoprotein s	71,597.40		-	-	7
9B	similar to Putative adenosylhomocysteinase 3	66,822.70		-	-	3

9C	Ubiquitin carboxyl-terminal hydrolase isozyme L1	24,820.20	27 kDa	3	4	5
9C	Triosephosphate isomerase	26,830.70		-	-	2
9C	Eukaryotic translation initiation factor 4H	27,306.90		-	3	3
9C	14-3-3 protein zeta/delta	27,753.90		-	-	2
9C	Inositol monophosphatase	30,493.60		-	4	2
9C	**Astrocytic phosphoprotein PEA-15**	**15,023.20**		**-**	**-**	**2**
9C	AU RNA binding protein/enoyl-Coenzyme A hydrata	33,324.10		-	2	-
9C	Enoyl-CoA hydratase, mitochondrial	31,499.50		-	-	2

9D	Hypoxanthine-guanine phosphoribosyltransferase	24,560.40	25 kDa	2	3	4
9D	Chloride intracellular channel protein 4	28,616.40		2	4	6
9D	**Ubiquitin carboxyl-terminal hydrolase isozyme L1**	**24,820.20**		**7**	**8**	**10**
9D	**Dihydropteridine reductase**	**25,534.30**		**4**	**4**	**8**
9D	Calretinin	31,388.70		7	6	11
9D	Isoform Crk-I of Proto-oncogene C-crk	22,845.80		-	-	4
9D	tetratricopeptide repeat domain 9	24,415.80		-	-	2
9D	coiled-coil domain containing 25	24,448.20		-	-	2
9D	**Astrocytic phosphoprotein PEA-15**	**15,023.20**		**-**	**-**	**2**
9D	Phosphoglycerate mutase 1	28,814.80		-	-	6

9I	Isocitrate dehydrogenase [NAD] subunit alpha, mitoc	39,596.40	35	4	4	6
9I	Fructose-bisphosphate aldolase A	39,334.50		3	4	3
9I	Fructose-bisphosphate aldolase C	39,266.30		9	4	3
9I	L-lactate dehydrogenase B chain	36,594.50		20	16	16

10A	Isoform 4 of Dynamin-1	97,571.50	99 kDa	17	32	26
10A	Isoform 8 of Dynamin-3	95,763.40		5	7	3
10A	Phosphorylase	96,759.10		2	8	2
10A	active BCR-related	97,678.50		-	2	2
10A	Hexokinase-1	102,392.90		-	3	6

10B	Plastin-3	70,664.50	75 kDa	9	12	8
10B	Isoform IA of Synapsin-1	73,970.30		6	11	17
10B	Heat shock cognate 71 kDa protein	70,854.70		13	23	27
10B	Stress-70 protein, mitochondrial	73,840.40		5	10	9
10B	ATPase, H+ transporting, lysosomal V1 subunit A	68,248.30		-	10	9
10B	Dihydropyrimidinase-related protein 1	74,232.00		-	3	6
10B	Dipeptidyl-peptidase 3	83,022.20		-	-	4

10C	Malate dehydrogenase, cytoplasmic	36,465.90		2	-	-
10C	Malate dehydrogenase, mitochondrial	35,666.20	35 kDa	3	-	-
10C	Mu-crystallin homolog	33,535.90		8	6	-
10C	L-lactate dehydrogenase B chain	36,594.50		14	13	7
10C	L-lactate dehydrogenase A chain	36,432.80		2	-	-
10C	N(G),N(G)-dimethylarginine dimethylaminohydrolas	31,407.90		2	-	-
10C	similar to glyceraldehyde-3-phosphate dehydrogenas	35,765.20		2	-	-
10C	WD repeat domain 54	35,575.90		2	-	-
10D	Thioredoxin-dependent peroxide reductase, mitochor	28,277.40	25 kDa	4	-	-
11A1	Fatty acid synthase	272,633.10	280kDa	20	38	9
11A2	Tln1 protein	271,021.00		-	2	-
11B	2-oxoglutarate dehydrogenase E1 component, mitoch	116,279.40	100 kDa	5	12	-
11B	Heat shock protein 105 kDa	96,400.50		-	3	4
11B	Ubiquitin-like modifier-activating enzyme 1	117,770.80		3	3	3
11B	Staphylococcal nuclease domain-containing protein 1	101,935.30		13	18	9
11B	Isoform Long of Clathrin coat assembly protein AP18	93,502.70		-	3	5
11B	Hexokinase-1	102,392.90		5	16	5
11B	alanyl-tRNA synthetase	106,795.70		7	18	3
11B	aminopeptidase puromycin sensitive	103,329.00		-	18	4
11B	**Isoform 1 of Synaptojanin-1**	**172,865.50**		**-**	**2**	**31**
11B	Isoform 4 of Dynamin-1	97,571.50		5	13	18
11B	Alpha-mannosidase 2C1	115,952.50		-	2	
11B	pitrilysin metallopeptidase 1	117,596.80		-	3	
11B	DnaJ (Hsp40) homolog, subfamily C, member 6	102,171.80		2	4	-
12A	1-phosphatidylinositol-4,5-bisphosphate phosphodie	138,330.20	140 kDa	7	12	12
12A	**Isoform 1 of Synaptojanin-1**	**172,865.50**		**17**	**22**	**19**
12A	Isoform Long of Clathrin coat assembly protein AP18	93,502.70		-	10	10
12A	**Isoform 1 of Neurofascin**	**137,987.60**		**-**	**3**	**3**
13A	ATP synthase subunit beta, mitochondrial	56,336.30	50 kDa	14	14	19
13A	Isoform Tau-E of Microtubule-associated protein tau	45,103.90		4	5	7
13A	Isoform IA of Synapsin-1	73,970.30		-	2	-
13A	Coronin-1A	51,046.90		-	2	2
13A	57 kDa protein	57,480.20		-	6	-
13A	Hsp90 co-chaperone Cdc37	44,492.30		-	-	3

14A	Filamin, alpha (Predicted), isoform CRA_a	281,264.10	280 kDa	4	-	-
14A	Alpha-1-inhibitor 3	163,756.40		19	16	23
14A	Fatty acid synthase	272,633.10		3	-	-
14A	Isoform 1 of Synaptojanin-1	172,865.50		9	7	11
14A	similar to Putative eukaryotic translation initiation fa	169,039.20		-	2	3
14A	filamin, beta	277,820.50		-	2	2
14A	**similar to talin 2**	**273,261.50**		**-**	**10**	**8**
17A	Serine/threonine-protein phosphatase 2A catalytic su	35,557.40	35 kDa	2	5	-
17A	**Alpha-soluble NSF attachment protein**	**33,175.80**		**4**	**8**	**3**
17A	Malate dehydrogenase, mitochondrial	35,666.20		4	6	3
17A	Succinyl-CoA ligase [GDP-forming] subunit alpha, n	36,130.50		6	6	3
17A	similar to N-ethylmaleimide sensitive fusion protein	39,874.30		7	10	6
17A	Pyruvate dehydrogenase E1 component subunit beta,	38,964.40		7	8	5
17A	35 kDa protein	34,641.80		-	4	3
17A	F-actin-capping protein subunit alpha-2	32,949.20		-	2	-
17A	Isoform Gamma-1 of Serine/threonine-protein phospl	36,967.60		-	2	-
17A	**Ubiquitin thioesterase OTUB1**	**31,252.50**		**-**	**4**	**-**
17B	Calcium-dependent secretion activator 1	146,250.50	150	2	3	10
17B	Non-erythroid spectrin beta	273,573.30		10	12	9
17B	Spectrin alpha chain, brain	284,697.80		82	108	91
17B	Non-erythrocyte beta-spectrin	251,192.50		67	74	69
17B	Spectrin beta chain, brain 2	271,047.30		-	2	-
17B	**Calpain-2 catalytic subunit**	**79,904.70**		**-**	**2**	**-**
17B	Leucine-rich PPR motif-containing protein, mitochon	156,641.70		-	-	2
17C	similar to ankyrin 2 isoform 2	210,668.30	280	6	3	-
17C	Spectrin alpha chain, brain	284,697.80		33	15	16
17C	Non-erythrocyte beta-spectrin	251,192.50		28	7	3
17C	Calcium-dependent secretion activator 1	146,250.50		-	5	10
17C	Isoform MAP2x of Microtubule-associated protein 2	202,393.40		-	2	-
17C	UDP-glucose:glycoprotein glucosyltransferase 1	176,576.50		-	-	21
18A	**Dynactin subunit 1**	**141,915.20**	**140**	**3**	**10**	**-**
18A	**Isoform 1 of Synaptojanin-1**	**172,865.50**		**-**	**2**	**5**
18A	Elongator complex protein 1	149,153.40		3	5	-
19A	**Amphiphysin**	**75 kDa**	**105 kda**	**24**	**12**	**29**
19A	**Isoform 2 of AP-2 complex subunit beta-1**	**105,676.60**		**4**	**8**	**9**
19A	Isoform 1 of Syntaxin-binding protein 1	67,553.80		4	4	6
19A	106 kDa protein	105,671.70		10	18	12
19A	**Ubiquitin carboxyl-terminal hydrolase**	**109,240.40**			**5**	**8**
19A	**Heat shock protein HSP 90-alpha**	**84,800.30**		**14**	**20**	**19**
19A	Isoform B of AP-1 complex subunit beta-1	103,857.70			5	
19A	Adaptor-related protein complex 2, alpha 2 subu	104,158.50			8	6
19A	Isoform MAP2x of Microtubule-associated prote	202,393.40				3
19A	Contactin-1	113,479.10				

19B	Cysteine and glycine-rich protein 1	20,595.20	20 kDa	2	-	2
19B	Cell cycle exit and neuronal differentiation protein 1	15,025.20		2	-	-
19B	COP9 signalosome complex subunit 8	23,218.10		-	-	3
19B	Isoform RTN1-S of Reticulon-1	23,540.20		-	-	2
20A	Isoform 1 of Syntaxin-binding protein 1	67,553.80	69 kda	9	14	14
20A	Heat shock cognate 71 kDa protein	70,854.70		26	29	25
20A	Stress-70 protein, mitochondrial	73,840.40		3	8	5
20A	**Microtubule-associated protein 1A**	**299,650.00**		**-**	**-**	**3**
20A	Isoform 1 of Microtubule-associated protein 6	100,466.20		-	-	2
20A	Isoform L-MAG of Myelin-associated glycoprotein	69,334.90		-	4	7
20B	Centaurin alpha	48,116.40	47 kDa	2	3	-
20B	similar to SH3-domain GRB2-like 2	52,375.10		4	9	13
20B	COP9 signalosome complex subunit 4	46,273.00		2	2	7
20B	2',3'-cyclic-nucleotide 3'-phosphodiesterase	47,252.00		11	18	18
20B	Creatine kinase B-type	42,708.10		-	2	3
20B	Cytochrome b-c1 complex subunit 2, mitochondrial	48,379.50		-	2	-
20B	Interleukin enhancer-binding factor 2	51,364.60		-	2	2
20B	succinate-Coenzyme A ligase, ADP-forming, beta sul	50,288.90		-	4	4
20B	Type II brain 4.1 minor isoform	107,053.90		-	-	2
20B	Probable saccharopine dehydrogenase	47,070.90		-	-	2
21A	Microtubule-associated protein 1A	299,650.00	290 kDa	8	14	15
21A	microtubule-associated protein 1B	269,625.40		3	20	24
21A	Isoform MAP2x of Microtubule-associated protein 2	202,393.40		5	17	15
21C	Prohibitin-2	33,295.60	37 kDa	4	10	6
21C	**microtubule-associated protein 1B**	**269,625.40**		**5**	**8**	**8**
21C	**Alpha-soluble NSF attachment protein**	**33,175.80**		**7**	**11**	**10**
21C	similar to glyceraldehyde-3-phosphate dehydrogenas	35,765.20		-	6	-
21C	COP9 constitutive photomorphogenic homolog subun	37,684.50		-	2	2
21C	**Microtubule-associated protein 1A**	**299,650.00**		**-**	**-**	**2**
21C	Isoform Gamma-1 of Serine/threonine-protein phospl	36,967.60		-	-	3
21C	Translation elongation factor 1-delta subunit	28,748.30		-	-	2
21C	Sideroflexin-3	35,415.30		-	-	2
21C	Electron transfer flavoprotein subunit alpha, mitocho	34,933.70		-	-	3
21C	Isoform 1 of NADH-cytochrome b5 reductase 3	34,157.80		-	-	2
21C	3-hydroxybutyrate dehydrogenase, type 1	38,315.60		-	-	2
21C	Lipid phosphate phosphohydrolase 3	35,301.90		-	-	2

During the rest of the project, we will select novel, most promising and non-redundant biomarker candidates, create immunoassay and validate in blast-induced model***: SOW3.***

Key Research Accomplishments:

- An accurate and highly reproducible model of blast exposure in rats has been validated.

- We achieved an independent control of rat exposure to OP peak only avoiding gas venting by varying the angle of animal location and distance from the nozzle of the shock tube. The precise calibration of the angle, distance and corresponding OP magnitude, duration and impulse has been achieved and tabulated.

- The high speed imaging reflected strong head acceleration upon on-axis head-directed blast, and minimal or no cervico-angular acceleration when rat is exposed to peak overpressure only (off-axis).

- GFAP and UCH-L1 have been demonstrated to be sensitive and specific biomarkers in serum of rats subjected to blast on-axis and off-axis. However, the pattern of release in circulation has shown to be different.

- The patterns of GFAP/UCH-L1 in CSF/blood following both on- and off axis blast exposure indicates a rapid blood-brain-barrier disruption/ restoration.

- Systemic, vascular, neuroinflammatory and neuroendocrine responses are essential components in responses to blast:

    - a/ When rats were exposed to peak OP through frontal region of the head w/o head accelleration, the levels of IL-1, IL-10, Selectins and chemokine Fractalkine response was higher than compared to head-directed exposure of a same magnitude: body protection decreased biomarkers release in circulation.
    - b/ similar profile of serum accumulation of Metalloproteinases has been detected.
    - c/ Resistin, adipose tissue hormone, and Orexin A, neuropeptide involved in energy balance exhibited comparable patterns of elevation in circulation.

- Beta-NGF has been shown to significantly elevate in serum after blast, may have neuroprotective/neurotrophic functions and be a marker of adaptive responses/neurorepair after blast induced TBI.
- Proteomic data have been obtained and are in the process of analysis and candidate biomarkers are in the process of selection. Currently, CNPase (determined in year 1), Orexin A and beta-NGF are potential candidates in addition to GFAP, UCH-L1 and spectrin-breakdown products.

Reportable Outcomes for the project period May 16, 2009-May 15, 2010

1. The review article entitled "**Biomarkers of Blast-Induced Neurotrauma: Profiling Molecular and Cellular Mechanisms of Blast Brain Injury"** by **Svetlov SI,** Larner SF, Kirk DR, Atkinson J, Hayes RL, Wang KK. has been published *J Neurotrauma* 2009 Jun, 26:1-9 **see Appendices**

2. The paper entitled "**Morphologic and biochemical characterization of brain injury in a model of controlled blast overpressure impact**" by **Svetlov SI,** Prima V, Kirk DR, Gutierrez H, Curley KC, Hayes RL, Wang KK. has been published in J Trauma. 2010 Oct;69(4):795-804. **see Appendices**

3. Abstract entitled **"Molecular and Cellular Fingerprints of Brain Overpressure Load: Potential Biomarkers of Blast Brain Injury"** by V. I. Prima[1], D. R. Kirk[2] , H. M. Gutierrez[2], M. V. Pereira[2], K. C. Curley[3], R. L. Hayes[1], K. W. Wang[1], **S. I. Svetlov[1]** was presented as poster at Advanced Technology Applications for Combat Casualty Care (ATACCC) 2009 St. Pete Beach, August 16-19, 2009 **see Appendices**

4. Abstract entitled '**Comprehensive Experimental Models for Profiling Mechanisms and Developing Biomarkers of Blast Brain Injury'** was presented at oral session by **Stanislav Svetlov** and Kevin Wang at Military Health Research Forum-2009, Kansas-City, MO , August 31-September 3, 2009 **see Appendices**

5. Abstract entitled "**Morphological and Biochemical Signatures of Brain Injury Following Head-Directed Controlled Blast Overpressure Impact'** by **Stanislav Svetlov**, Victor Prima, Daniel Kirk, Joseph Atkinson, Hector Gutierrez, Kenneth Curley, Ronald Hayes, Kevin Wang was presented as poster at 27th Annual National Neurotrauma Symposium, September 7-11, 2009, Santa Barbara CA. **see Appendices**

Conclusion

In the second year of the project, we completed validation of both models of 'composite' blast exposure with controlled parameters of blast wave impact on axis and exposure to 'pure' Overpressure Peak (primary blast). According to SOW2 (tasks 4, 5), we demonstrate GFAP and UCH-L1 to be sensitive biomarkers after exposure to both composite and primary blast, however with different patterns. We demonstrate that systemic (IL-1, IL-10, Fractalkine), vascular (selectins) and neuroendocrine (Resistin, Orexin A) responses to blast are most prominent when frontal region of rat head is exposed to OP without significant head acceleration. Experimental evidence has been obtained that beta-NGF may be involved in adaptive responses/neurorepair after blast-induced TBI. Using targeted proteomics, we identified a number of proteins up- or down-regulated in midbrain after blast. Detailed mechanisms and selection of novel non-redundant biomarkers of blast exposure, particularly primary blast, will be accomplished from later in the course of project and corresponding immunoassay (s) developed.

References:

1. **Svetlov SI,** Larner SF, Kirk DR, Atkinson J, Hayes RL, Wang KK. has been published *J Neurotrauma* 2009 Jun, 26:1-9
2. **Svetlov SI,** Prima V, Kirk DR, Gutierrez H, Curley KC, Hayes RL, Wang KK. Morphologic and Biochemical Characterization of Brain Injury in a Model of Controlled Blast Overpressure Exposure. J Trauma. 2010 Oct;69(4):795-804
3. Stuhmiller JH, Ho KH, Vander Vorst MJ, et al. A model of blast overpressure injury to the lung. *J Biomech* 1996;29:227-234.
4. Jaffin JH, McKinney L, Kinney RC, et al. A laboratory model for studying blast overpressure injury. *J Trauma* 1987;27:349-356.
5. Atkinson JP, Faure JM, Kirk DR, et al. Generation and Analysis of Blast Waves from a Compressed Air-Driven Shock Tube. The American Institute of Aeronautics and Astronautics (AIAA) Journal 2010;In press.
6. Guy RJ, Kirkman E, Watkins PE, et al. Physiologic responses to primary blast. *J Trauma* 1998;45:983-987.
7. Cooper PW. Explosives Engineering. Wiley-VCH; 1996.
8. Saljo A, Bao F, Haglid KG, et al. Blast exposure causes redistribution of phosphorylated neurofilament subunits in neurons of the adult rat brain. J Neurotrauma 2000;17:719-726.
9. Elsayed NM. Toxicology of blast overpressure. Toxicology 1997;121:1-15.
10. Stuhmiller JH. Biological response to blast overpressure: a summary of modeling. Toxicology 1997;121:91-103.
11. Svetlov SI, Larner SF, Kirk DR, et al. Biomarkers of Blast-Induced Neurotrauma: Profiling Molecular and Cellular Mechanisms of Blast Brain Injury. *J Neurotrauma* 2009, 26:1-9
12. de Olmos JS, Beltramino CA, de Olmos de Lorenzo S. Use of an amino-cupric-silver technique for the detection of early and semiacute neuronal degeneration caused by neurotoxicants, hypoxia, and physical trauma. *Neurotoxicol Teratol* 1994;16:545-561.
13. Switzer RC, 3rd. Application of silver degeneration stains for neurotoxicity testing. *Toxicol Pathol* 2000;28:70-83.
14. Kupina, N.C., Nath, R., Bernath, E.E., Inoue, J., Mitsuyoshi, A., Yuen, P.W., Wang, K.K., and Hall, E.D. (2001). The novel calpain inhibitor SJA6017 improves functional outcome after delayed administration in a mouse model of diffuse brain injury. J Neurotrauma *18*, 1229-1240.
13. Galea, E., P. Dupouey and D. L. Feinstein (1995). "Glial fibrillary acidic protein mRNA isotypes: expression in vitro and in vivo." J Neurosci Res **41**(4): 452-461.
14. Urrea C, Castellanos DA, Sagen J, et al. Widespread cellular proliferation and focal neurogenesis after traumatic brain injury in the rat. *Restor Neurol Neurosci* 2007;25:65-76.
15 Nylen K, Ost M, Csajbok LZ, et al. Increased serum-GFAP in patients with severe traumatic brain injury is related to outcome. *J Neurol Sci* 2006;240:85-91.
16. Kaur, C., J. Singh, M. K. Lim, B. L. Ng and E. A. Ling (1997a). "Macrophages/microglia as 'sensors' of injury in the pineal gland of rats following a non-penetrative blast." Neurosci Res **27**(4): 317-322.

APPENDICES:

JOURNAL OF NEUROTRAUMA 26:913–921 (June 2009)

DOI: 10.1089/neu.2008.0609

Biomarkers of Blast-Induced Neurotrauma: Profiling Molecular and Cellular Mechanisms of Blast Brain Injury

Stanislav I. Svetlov,[1,3] Stephen F. Larner,[1] Daniel R. Kirk,[2] Joseph Atkinson,[2] Ronald L. Hayes,[1] and Kevin K.W. Wang[1,4]

Abstract

The nature of warfare in the 21st century has led to a significant increase in primary blast or over-pressurization injuries to the whole body and head, which manifest as a complex of neuro-somatic damage, including traumatic brain injury (TBI). Identifying relevant pathogenic pathways in reproducible experimental models of primary blast wave exposure is therefore vital to the development of biomarkers for diagnostics of blast brain injury. Comparative analysis of mechanisms and putative biomarkers of blast brain injury is complicated by a deficiency of experimental studies. In this article, we present an overview of current TBI biomarkers, as well as outline experimental strategies to investigate molecular signatures of blast neurotrauma and to develop a pathway network map for novel biomarker discovery. These biomarkers will be effective for triaging and managing both combat and civilian causalities.

Key words: biomarkers; blast; brain injury; molecular pathways; traumatic brain injury

Introduction

An understanding of the biological mechanisms, and particularly the biomarkers of blast-induced neurotrauma, remain elusive. Symptoms of blast brain injury often do not manifest themselves until sometime after the injury has occurred (Cernak et al., 1999a; Yilmaz and Pekdemir, 2007). Mild or moderate brain injuries in particular often go undiagnosed and untreated because emergency medical attention is directed toward more visible injuries such as penetrating flesh wounds (Belanger et al., 2005; Lew, 2005). However, even mild and moderate brain injuries can produce significant deficits, and when repeated can lead to sustained neuro-somatic damage and neurodegeneration (Lew, 2005; Lew et al., 2005).

Over the last several decades, a number of experimental animal models have been implemented to study the mechanisms of blast wave impact and include rodents and larger animals such as sheep (Savic et al., 1991; Stuhmiller et al., 1996). Shock tubes have been used as the fundamental research tool for the past several decades. However, because of the rather generic nature of the blast generators used in the different studies, the data on injury mechanisms, including brain damage, have been difficult to analyze and compare (Jaffin et al., 1987; Elsayed 1997; Guy et al., 1998). Thus, there is still a lack of relevant reproducible models within the blast injury framework, including the development of generators that precisely control parameters of the blast wave, similarly to those present in classical mechanical controlled cortical impact (CCI) models. This makes it difficult to investigate the blast injury mechanisms and to develop relevant biomarkers for diagnostics and mitigation. However, preliminary analysis of the data on blast brain injury mechanisms suggests that it can be compared to the CCI injury model and potential biomarkers suggested by the latter can be examined.

The goals of this review are to examine potential biochemical/pathophysiological pathways and possible biomarkers of blast brain injury.

Review of Existing Biomarker Candidates

According to a generally accepted definition, a biomarker has the characteristic that it can be objectively measured

[1]Center of Innovative Research, Banyan Biomarkers, Inc., Alachua, Florida.
[2]Department of Mechanical and Aerospace Engineering, Florida Institute of Technology, Melbourne, Florida.
[3]Departments of Physiological Sciences and [4]Psychiatry, University of Florida, Gainesville, Florida.

and evaluated as an indicator of normal biological processes, pathogenic processes, or pharmacological responses for therapeutic intervention (Biomarkers Definitions Working Group, 2001). In contrast, a "surrogate biomarker" or "surrogate endpoint" is expected to predict clinical effects based on therapeutic, pathophysiologic, or other scientific correlations. Despite the apparent consensus on definition, controversy still exists about how to clearly delineate these two groups that have been associated with different experimental approaches that employ biomarkers for discovery and validation (Lescuyer et al., 2007). Ideally, brain injury biomarkers should be biological substrates unique to the brain and should provide information on injury mechanisms, a criterion used to distinguish biochemical markers from surrogate markers of injury, since surrogate markers usually do not provide information on injury mechanisms. Although there are currently no biomarkers with proven clinical utility for the diagnosis of brain injury, whether caused by blast, mechanical trauma, stroke, or other acute brain injuries, research has uncovered several valuable candidates that have shown preclinical potential. The ones currently generating the most interest include S-100ß, neuron specific enolase (NSE), glial fibrillary acid protein (GFAP), and myelin basic protein (MBP). Although these proteins are still being assessed, they appear to lack either the necessary sensitivity or brain specificity (except perhaps GFAP) to be used effectively alone (Bazarian et al., 2006; Piazza et al., 2007). However, the combination of these markers can effectively detect TBI and provide outcome predictions (Berger et al., 2005; Berger et al., 2007). Below is a brief analysis of these generally accepted putative biomarkers of TBI.

S-100ß protein

S-100ß is among the most well studied proteins for TBI and is considered a promising, non-proprietary brain injury biomarker. S-100ß, a small dimeric calcium binding protein, is most abundant in glial cells of the central nervous system (astrocytes) and peripheral nervous system (Schwann cells). A weakness of this marker is that it is not exclusive to the brain; S-100ß has been found to be expressed in melanocytes, adipocytes, and chondrocytes (Michetti and Gazzolo, 2002).

A number of studies have demonstrated S-100ß's relationship to injury magnitude and outcome in TBI (Pelinka et al., 2004; Berger et al., 2005; Berger et al., 2007; Korfias et al., 2007). This suggests that S-100ß may be useful in assessing the efficacy of treatment after severe TBI (Korfias et al., 2007). Other studies, however, reported a poor value of S100ß as a predictor of outcome after brain injury, particularly mild and pediatric TBI (Bazarian et al., 2006; Kleindienst and Bullock, 2006; Piazza et al., 2007). Also, several studies raised concern whether the serum level of S100ß can be considered a true biochemical marker of brain damage given the definition of "biomarker" discussed above (see Kleindienst et al., 2007 for review). For example, in several studies a poor correlation was found between serum and brain S100ß values, suggesting that the serum levels may depend primarily on the integrity of the blood–brain barrier and do not reflect the S100ß levels in the brain (Kleindienst and Bullock, 2006; Piazza et al., 2007). Despite apparent controversy, S-100ß still has potential as a brain injury biomarker, and its preclinical and clinical utility should be further explored, especially after blast wave exposures.

Neuron specific enolase

NSE initially held promise as a brain injury biomarker, as it was originally believed to be strictly neuronal. The protein is located in the neuronal cytoplasm and is involved in regulating intracellular chloride levels (Vinores et al., 1984). However, follow-up research found that NSE is also present in red blood cells and platelets, decreasing its diagnostic utility as a marker due to possible cross-contamination that could occur in blood samples (Johnsson et al., 2000). In clinical studies, serum NSE levels have been frequently studied alongside S-100ß. The sensitivity and specificity of serum NSE after pediatric TBI as determined by ROC curves was found to be 71% and 64%, respectively (Berger et al., 2005). After multiple trauma, elevated NSE levels have been observed, but systemic NSE increased by similar degrees with and without TBI, limiting its ability to discriminate brain injury magnitude (Pelinka et al., 2005). Additionally, NSE has a long half-life, more than 20 h in serum, and this may account for its limitation for use as a TBI biomarker (Ingebrigtsen and Romner, 2003). Reports on correlations of serum NSE levels alone with clinical and neurological measures of brain injury magnitude and overall outcome have been controversial (Berger et al., 2005; Berger et al., 2007; Ingebrigtsen and Romner, 2003; Pelinka et al., 2005), although assay of serum NSE together with S100ß have been valuable in predicting TBI outcome (Berger et al., 2006; Berger et al., 2007).

Glial fibrillary acidic protein

Glial fibrillary acidic protein (GFAP), a filament protein found in the astroglial cytoskeleton, is not found outside the CNS (Galea et al., 1995). It has only recently gained attention as a TBI biomarker, when it was shown to be as good as if not more promising than S-100ß. In a study of 92 severe TBI patients both GFAP and S-100ß were shown to be equally good predictors of mortality, with sensitivity between 70% and 84% depending on the time they were measured after injury (Pelinka et al., 2004; Nylen et al., 2006). In addition to discriminating survival after TBI, GFAP, but not S-100ß, could predictably discriminate between severe disability and vegetative state versus good and moderate outcomes as evaluated by the Glasgow Outcome Scale (GOS). Another study of 114 severe TBI patients confirmed its ability to predict mortality (Pelinka et al., 2004), and it was found to further discriminate outcome categories of the GOS. This study also indicated that GFAP had the ability to discriminate injury severity based on the Marshall scale classification of computed tomography (CT) scans. It could discriminate between patients that had intracranial pressure (ICP) greater or less than 25 mm Hg, patients that had cerebral perfusion pressure greater or less than 60 mm Hg, and patients with mean arterial pressure greater or less than 60 mm Hg. In a third study of 85 patients with severe TBI, levels of GFAP, NSE, and S-100ß taken on hospital admission correlated with outcome measured by GOS at 6 months. Biomarker levels also correlated moderately with other indices of injury magnitude and were better correlated with Glasgow Coma Scale scores than was CT scan analysis. GFAP shows good diagnostic potential to predict outcome after injury, and may also be valuable for diagnosing

injury magnitude, although it has not been studied in mild and moderate injury. Since it appears to be specific for brain tissue and is not affected by hemorrhagic shock or extracranial trauma, it may be a better diagnostic tool than S-100ß.

Myelin basic protein

Myelin basic protein (MBP), an abundant protein in white matter, has been examined as a marker of axonal damage in several insults germane to neurointensive care. In TBI, CSF and serum levels of MBP have demonstrated excellent specificity, but limited sensitivity (Berger et al., 2005). It was recently shown that serum MBP, as well as NSE and S100β, concentrations obtained at the time of TBI may be useful in predicting outcome after pediatric TBI (Berger et al., 2006; Berger et al., 2007).

More recently a number of new candidate biomarkers have been discovered. The emerging data suggest TAU (c-tau) proteins (Zemlan et al., 2002; Gabbita et al., 2005), αII-spectrin protein breakdown products (SBDPs) (Pike et al., 1998a; Pike et al., 1998b; Pike et al., 2001; Pineda et al., 2004; Haskins et al., 2005; Wang et al., 2005; Kobeissy et al., 2006; Ottens et al., 2006; Pineda et al., 2007), and other proteins have strong potential. Currently, Banyan Biomarkers, Inc. is performing ELISA validation on some of these markers, and clinical validation of the biomarkers with human serum samples is in progress.

Microtubule associated protein-tau (c-Tau)

The same enzymes that cleave the cytoskeletal protein αII-spectrin cleave the microtubule associated protein-tau, releasing breakdown products (BDPs) with molecular weights that profile cleavage activity as being induced by the pro-necrotic calpains or the pro-apoptotic caspases. Tau cleavage by calpains include a BDP at 17 kDa that has been noted in cells following ß-amyloid peptide treatment (Park and Ferreira, 2005; Park et al., 2007). Caspases have been shown to produce a tau breakdown product (TBDP) around 45 kDa (Chung et al., 2001). TBDPs were found to be present after TBI in rats (Zemlan et al., 2002; Gabbita et al., 2005). In a study whose primary objective was to determine the relationship between serum S-100ß and c-tau levels and long-term outcome after mild TBI, S-100ß and c-tau levels in serum taken 6 h after injury for 35 mild TBI subjects were compared to 3-month post-TBI Rivermead Post Concussion Questionnaire (RPCQ) scores and post-concussive syndrome. The results showed a weak linear correlation between marker levels and RPCQ scores for both markers, and that there was no statistically significant correlation between marker levels and 3-month post-concussive syndrome. Thus, serum S-100ß and c-tau levels are apparently poor predictors of 3-month outcome after mild TBI (Bazarian et al., 2006). Further studies are required to ascertain whether the MAP-tau protein is a valid biomarker for brain trauma.

αII-Spectrin breakdown products

αII-spectrin is a major structural component of the neuron axonal cytoskeleton and a major proteolytic substrate for cysteine proteases (calpain and caspase-3) involved in oncotic (necrotic) and apoptotic cell death, respectively (Wang et al., 1998). Considerable evidence has been accumulated by our laboratory that αII-spectrin possesses signature cleavage products with molecular weights of 150 (SBDP150) and 145 kDa (SBDP145) due to cleavage by calpain, and a transient fragment of 150 kDa (SBDP150i) and a major cleavage product of 120 kDa (SBDP120) by caspase-3 (Nath et al., 1998; Pike et al., 1998a; Pike et al., 1998b). Since calpains and caspases become hyperactivated after traumatic and ischemic brain injury, we have proposed that SBDPs would be useful biomarkers of brain injury. Indeed, we and others found that these signature cleavage products are apparent in brain tissue and CSF after brain injury in rats (Pike et al., 1998a; Beer et al., 2000; Pike et al., 2001), brain ischemia (Zhang et al., 2002), and in human CSF following TBI (Pineda et al., 2004; Ringger et al., 2004). While MBP and c-Tau are relatively specific to the brain, the cytoskeleton αII-spectrin and its cleavage products SBDP150, 145, and 120 are not. Thus, plasma/serum levels of αII-spectrin SBDPs reflect the magnitude of multi-organ damage (including brain) rather than TBI per se.

NMDA-R fragments

Potential biomarkers for brain injury may include the fragmented form of the glutamate-*N*-methyl-D-aspartate (NMDA) receptor (NR2A/2B subtype). Dambinova and colleagues investigated the diagnostic accuracy of serum autoantibodies to NR2A/2B, a subtype of NMDA receptor, in assessing transient ischemic attack (TIA) and ischemic stroke (IS), and its ability to distinguish cerebral ischemia from intracerebral hemorrhage (ICH). They showed that patients with TIA ($n = 56$) and acute IS ($n = 31$) had significantly higher NR2A/2B autoantibody concentrations than controls. In addition, levels of NR2A/2B autoantibodies within 72 h in the IS group differed significantly from those in ICH patients ($p < 0.001$). This was confirmed by magnetic resonance imaging and CT (Dambinova et al., 2003). It was concluded that NR2A/2B autoantibodies are independent and sensitive serologic markers capable of detecting TIA with a high post-test probability, and this correlates well with neurologic observation and neuroimaging, thereby ruling out ICH. Also, this biomarker may help assess the risk of TIA in routine general practice, and may potentially be useful in assisting diagnosis of acute IS in the emergency setting.

Neuro-inflammatory cytokine markers

The role of inflammation in various CNS injuries has been shown in numerous studies (see Lucas et al., 2006 for review). Hayakata and associates investigated early changes in the concentrations of CSF S-100β and various cytokines after TBI, and evaluated the relations of both to ICP and prognosis. CSF concentrations of S-100β and CSF and serum concentrations of five cytokines (IL-1β, TNF-α, IL-6, IL-8, and IL-10) were measured and compared. The CSF concentrations of S-100β and the cytokines peaked within 24 h after severe TBI, and decreased gradually thereafter. The authors concluded that CSF S-100β and IL-1β may be useful as outcome predictors in cases of severe TBI (Hayakata et al., 2004). In a subsequent study, they compared the CSF and serum levels of pro- and anti-inflammatory cytokines in 35 patients with severe TBI with and without additional injury. CSF and serum concentrations of two pro-inflammatory mediators (IL-1β and TNF-α), and three anti-inflammatory mediators (IL-1 receptor

antagonist [IL-1ra], soluble TNF receptor-I [sTNFr-I], and IL-10) were measured and compared at 6 h after injury. CSF concentrations of pro-inflammatory mediators were much higher than the corresponding serum concentrations in both patient groups. In contrast, serum concentrations of anti-inflammatory mediators were much higher than the paired CSF concentrations in patients with additional injury, but serum concentrations were lower than or equal to the corresponding CSF concentrations in patients without additional injury. CSF concentrations of IL-1β, IL-1ra, sTNFr-I, and IL-10 were significantly higher in patients with high ICP than in patients with low ICP, and were also significantly higher in patients with an unfavorable outcome than in patients with a favorable outcome. These studies suggest that increased serum concentrations of anti-inflammatory mediators after severe TBI were mainly due to the additional extracranial injury/polytrauma. In contrast, anti-inflammatory mediators in CSF may be useful indicators of the severity of brain damage in terms of ICP, as well as overall prognosis of patients with severe TBI (Shiozaki et al., 2005).

General Approaches for Studies of Specific Mechanisms of Blast-Related Injuries

In the blast injury model, experimental animals are exposed to blasts that result from the detonation of known quantities of explosives at varying distances from the source, at different body orientations towards the blast wave, and in open or confined fields (Elsayed, 1997; Axelsson et al., 2000; Saljo et al., 2000). Also, a number of investigations have employed compressed air-driven shock tubes and nitrogen-driven blast wave generators to expose various animals to blast injury (e.g., rats, mice, and rabbits) to analyze the mechanisms of injury (Jaffin et al., 1987).

The majority of the blast injury–related work has been done using animals that have been exposed to total body blasts (Cernak et al., 1991a; Cernak et al., 1991b; Cernak et al., 1995; Stuhmiller et al., 1996; Elsayed, 1997; Elsayed et al., 1997; Gorbunov et al., 1997; Januszkiewicz et al., 1997; Mayorga, 1997; Cernak et al., 1999c; Cernak et al., 2001a; Elsayed and Gorbunov, 2003; Chavko et al., 2006; Elsayed and Gorbunov, 2007). Several groups reported that animals exhibited lung and abdominal injuries when they were exposed to a directed shock tube–generated blast. Guy and co-workers showed that rats exposed to moderate thoracic blast exhibited increased apnea, bradycardia, and hypotension before they returned to pre-blast values. No significant cardiovascular or respiratory changes were seen in animals subjected to abdominal blast (Guy et al., 1998). The most noticeable damage after blast exposure was found in the inner ear, lungs, and other gas- or fluid-containing interfaces such as the gastrointestinal tract (Cernak et al., 1991a; Cernak et al., 1991b; Elsayed, 1997; Elsayed et al., 1997; Januszkiewicz et al., 1997; Chavko et al., 2006; Elsayed and Gorbunov, 2007).

Several reports suggest that free radical–mediated injury in lung and blood of rats, rabbits, and sheep occurs in response to the blast (Elsayed et al., 1996, 1997). The biochemical changes included an increase in lipid peroxidation and hemoglobin associated with decreased Pao_2, and antioxidant depletion and impairment of calcium transport across the cell membrane. These changes were found to correlate well with blast peak overpressure (Elsayed et al., 1996).

Hemoglobin and especially either of its oxidation products (metHb and oxoferrylHb) or its degradation products (heme and free iron) promote injury due to free radical–mediated consequences (Elsayed et al., 1996; Gorbunov et al., 1997). This may explain the continued pathological response after the blast wave exposure has ceased. Nitric oxide (NO) released from endothelial cells can form ligands that complex the active iron on the hemoglobin molecules rendering it unreactive (i.e., NO may function as an antioxidant by quenching the hemoglobin-mediated free-radical reactions) (Gorbunov et al., 1996). On the other hand, following blast exposure, endogenous NO was observed to increase in some rat tissues including lung and brain tissue.

Identification of brain-specific blast injury mechanisms and potential biomarkers

Several decades of medical literature reports provide a number of cases in which brain injuries are likely to have resulted from primary blast forces (Cramer et al., 1949; Murthy et al., 1979). Reported neuropathological changes have included small hemorrhages within the white matter, chromatolytic changes in the neurons (due to degeneration of Nissl bodies, an indication of neuronal damage), diffuse brain injury, and subdural hemorrhage. It is still controversial whether primary blast forces directly damage the brain, and if they do, what the mechanisms are that mediate the injury (Taber et al., 2006).

Shear and stress waves from the primary blast could potentially cause TBI directly (e.g., concussion, hemorrhage, edema, and diffuse axonal injury). On the other hand, the primary blast can also cause formation of gas emboli, leading to infarction (Guy et al., 2000a; Guy et al., 2000b).

The most common types of TBI are diffuse axonal injury, contusion, and subdural hemorrhage (Vander Vorst et al., 2007). Diffuse axonal injuries are very common following closed head injuries. They result when shearing, stretching, and/or angular forces pull on axons and small vessels. Impaired axonal transport leads to focal axonal swelling and after several hours may result in axonal disconnection (Hurley et al., 2004). The most common locations are the corticomedullary (gray matter-white matter) junction (particularly in the frontal and temporal areas), the internal capsule, the deep gray matter, the upper brainstem, and the corpus callosum. However, it has been shown that severely injured axons do not necessarily swell. The presence of focal axonal swellings, the most commonly used neuropathological marker for TBI, may therefore seriously underestimate the magnitude of injury present. It has also been noted that the insensitivity of presently used neuropathological markers to the unmyelinated fine-caliber axons that make up 30% of the corpus callosum may also contribute to inaccurate injury evaluation. After rats had been exposed to a total body blast, a phosphorylated epitope of the heavy subunit of the neurofilament proteins (p-NFH) normally restricted to axons, accumulated in the neuronal perikarya in layers II–IV of the temporal cortex, and in the piriform cortices, the dentate gyrus, and the CA1 region of the hippocampus. At the same time, the p-NFH immunoreactivity disappeared from the axons and dendrites of cerebral cortex neurons. These findings suggested a dephosphorylation of NFHs in axons and dendrites, and an accumulation of p-NFHs in the perikarya due to disturbed

axonal transport (Saljo et al., 2000). The authors noted that these changes are likely the result of disturbed anterograde axonal transport.

Cernak and co-workers studied the effect on the brain of exposure to primary blast (delivered by a shock tube) and noted that it was sufficient to cause a moderate level of lung injury in rats (Cernak et al., 1999b; Cernak et al., 2001a, 2001b). In some cases, the effect of exposing the whole body was compared to exposing only the thoracic region (with the head protected) (Cernak et al., 2001b). Both types of blast exposure resulted in ultrastructural evidence of neuronal injury (expanded perineuronal spaces, cytoplasmic vacuoles, myelin deformation, and axoplasmic shrinkage) in the areas examined (hippocampus and brainstem reticular formation). The authors noted that the pattern of neuronal abnormalities is similar to those seen in diffuse axonal injury. Biochemical changes indicative of oxidative stress were also present. The degree of neuronal damage correlated with impaired performance on an active avoidance task (Cernak et al., 1999b; Cernak et al., 2001a, 2001b).

In a recent controversial paper, Kato and co-workers exposed rats to a direct single shock-wave shot (produced by a silver azide explosion) after craniotomy. This high-overpressure (>10 MPa) shock-wave exposure resulted in hemorrhage and a significant increase in TUNEL-positive neurons exhibiting chromatin condensation, nuclear segmentation, and apoptotic bodies. The maximum increase was seen at 24 h after the shock-wave application. Low-overpressure (1 MPa) shock-wave exposure resulted in spindle-shaped changes in neurons and elongation of nuclei without marked neuronal injury. The administration of the caspase-3 antagonist Z-VAD-FMK significantly reduced the number of TUNEL-positive cells observed 24 h after high-overpressure shock-wave exposure. High-overpressure shock-wave exposure results in brain injury, including neuronal apoptosis mediated by a caspase-dependent pathway. The authors speculated that the threshold for shock-wave–induced brain injury is under 1 MPa, a level that is lower than the threshold for other organs including lungs (Kato et al., 2007). However, the model of blast injury employed in this study is very similar to a controlled cortical impact (CCI) model, which our group has been using for a number of years in rat TBI studies (Pineda et al., 2004; Wang et al., 2005; Ottens et al., 2006). Specifically, Kato and colleagues imposed the pressure of blast wave locally on dura mater after craniotomy instead of using mechanical piston impact at various depths as is typical in our studies. It is not clear from the study whether the magnitude and duration of overpressure blast was measured at the surface of the dura mater. The morphological pattern of brain tissue injury in that model closely resembled the damage observed after CCI (Kato et al., 2007).

In a number of studies using a CCI model of TBI in rats, we have convincingly demonstrated the important role for caspase-3-mediated apoptotic pathways in neuronal injury, as well as the calpain-mediated oncosis/necrosis mechanisms (Pineda et al., 2004; Wang et al., 2005; Ottens et al., 2006). Several pathways and target proteins have been identified as potential biomarkers of TBI (Kobeissy et al., 2006). Moreover, a systems biology approach was implemented to construct a network map of proteins and pathways involved in the pathophysiology of TBI (Kobeissy et al., 2006). Whether these pathways are equally critical after blast-wave exposure of total body and/or direct head targeting without imposing mechanical/traumatic forces remains to be elucidated.

Importantly, the rats exposed to blast injury exhibited significant deficits in performance of an active avoidance task that persisted up to 5 days post-injury. Electron microscopy findings in several brain structures showed swellings of neurons, glial reaction, myelin debris, and increased pinocytotic

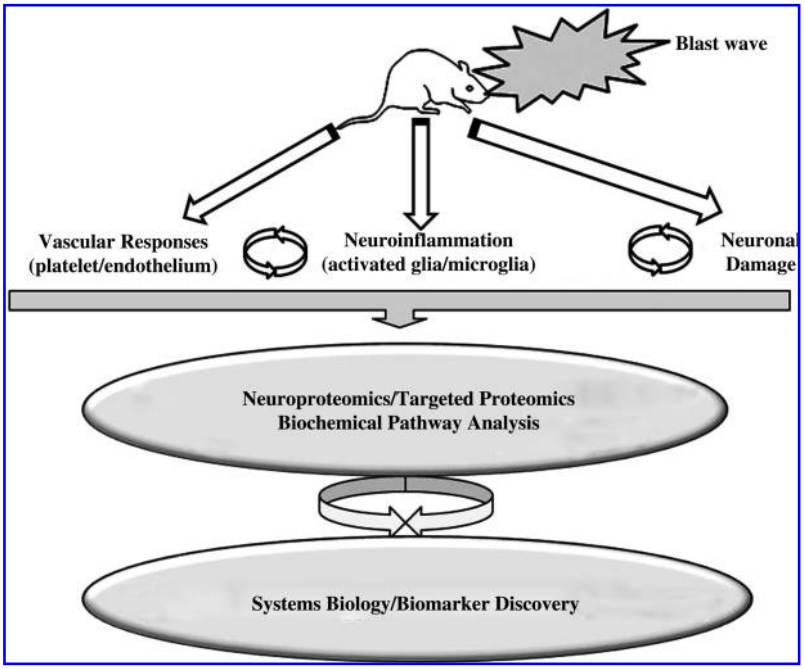

FIG. 1. Schematic presentation of a proposed research algorithm to elucidate molecular signatures and pathophysiological pathways of blast brain injury to develop a network map for blast brain injury.

activity on the fifth day following trauma. In blast-injured rats, there was also a significant elevation in total nitrite/nitrate levels 3 and 24 h following injury, which were comparable with the changes in the expression of inducible nitric oxide synthase mRNA. The results indicate that blast injury–induced neurotrauma is able to cause cognitive deficits (Cernak et al., 2001a). In a later study, performance tests of coordination, balance, and strength were significantly impaired by exposure to a more intense explosion. An increase in the number of degenerating neurons was seen in cerebral cortex following these more intense explosions (Moochhala et al., 2004). An important finding was that administration of aminoguanidine, an antagonist of inducible NO synthase, before or after blast exposure ameliorated the blast-evoked behavioral changes (Moochhala et al., 2004).

On the other hand, as indicated above, NO may function as an antioxidant by quenching the hemoglobin-mediated free-radical reactions (Gorbunov et al., 1996). Thus the roles of NO and NO synthase, and particularly iNOS, in blast brain injury remains unclear. Moreover, recent studies using spin trap techniques and nitrosylation markers in iNOS knockout mice indicated that NO may play a dual role after TBI, that is both injurious and protective, depending on the time after traumatic impact (Bayir et al., 2005; Foley et al., 2008).

For rats subjected to an explosive-generated blast, Kaur and co-workers showed generalized activation of microglia and astrocytes 1 and 7 days after the blast, particularly in the superficial layers of the cerebral and cerebellar cortices, while the oligodendrocyte profile remained intact (Kaur et al., 1995, 1996, 1997a, 1997b, 1999). It was concluded from this study that the blast may have disrupted the integrity of the blood–brain barrier, resulting in possible abnormal entry of serum-derived substances, thereby leading to microglia/astrocytic activation.

Approaches for the development of specific biomarkers of blast-induced brain injury

Integrating the existing data obtained from different models of blast brain injury, as well as from classical CCI-like models, we propose that exposures to blast waves cause brain injury with distinct biochemical pathophysiological signatures, which when defined and integrated with systems biology tools, can be exploited to discover diagnostic biomarkers and blast brain injury mitigation strategies. For example, we recently employed Pathway Studio software for creation of a functional interaction map of proteins affected during controlled cortical impact TBI (Kobeissy et al., 2006). We propose the term BLAST-OMICS for the similar functional interaction map of proteins impacted by blast-wave exposure, which will be created during current and future studies.

We postulate that the following molecular pathways and/or targets are identifiable upon blast wave exposures of experimental animals (Fig. 1).

1. Vascular responses and dysregulation of cell adhesion molecules as bridges connecting vascular-endothelial-neural tissue disturbances, including but not limited to nitric oxide metabolism assessed in brain tissues, CSF, and blood by Western blot, sandwich ELISA, and immunohistochemical means.
2. Neuroinflammation as a further development of impaired vascular reaction in the brain, resulting in enhancement of endothelial permeability/leakage, infiltration of macrophages, and activation of microglia that will involve cytokines and markers of activated microglia.
3. Neuron-glia interactions and cell death pathways, including apoptosis, oncosis/necrosis, and autophagy.
4. Additional pathways and biomarkers, such as dendrite/axonal disturbances including axonal transport dysfunction and damage to microtubules and neurofilaments.

The successful development of true biochemical markers of blast brain injury should help to distinguish between minor brain damage, particularly mild TBI, and post-traumatic stress disorder (Kennedy et al., 2007; King, 2008). The differentiation of PTSD and mild TBI is especially important for soldiers returning from Iraq, as mild TBI (e.g., concussion) that occurs among these soldiers has a strong association with PTSD and physical health problems 3 to 4 months after the soldiers return home (Hoge et al., 2008).

Perspectives

Despite a long history, critical need, and a vast array of recent data, the mechanisms of primary blast neurotrauma, particularly brain injury and potential biomarkers, remain elusive. A lack of unified models with defined blast-wave signatures has contributed significantly to existing controversies. Given data from both our laboratory and others, it has become increasingly clear that brain pathology, the underlying mechanisms and potential biomarkers associated with primary blast exposures, may be different from those imposed by focal mechanical head trauma (Bhattacharjee, 2008). This exciting new area of research clearly requires more adequate models and in-depth studies of biochemical/pathophysiological signatures of blast neurotrauma. Thus the design and implementation of a relevant experimental framework is of particular importance for elucidation of the mechanisms of injury, the identification of biomarkers, and eventually the development of strategies for mitigating blast-induced brain injury.

Acknowledgments

The authors wish to thank Ms. Qiushi Tang for her excellent technical assistance. This work was supported by grants N14-06-1-1029, W81XWH-8-1-0376 and X81XWH-07-01-0701 from Department of Defense.

Author Disclosure Statement

Dr. Svetlov, Dr. Larner, Dr. Hayes, and Dr. Wang have financial interest in Banyan Biomarkers Inc. Dr. Kirk and Dr. Atkinson have no conflict of interests.

References

Axelsson, H., Hjelmqvist, H., Medin, A., Persson, J.K., and Suneson A. (2000). Physiological changes in pigs exposed to a blast wave from a detonating high-explosive charge. Mil. Med. 165, 119–126.

Bayir, H., Kagan, V.E., Borisenko, G.G., Tyurina, Y.Y., Janesko, K.L., Vagni, V.A., Billiar, T.R., Williams, D.L., and Kochanek, P.M. (2005). Enhanced oxidative stress in iNOS-deficient mice after traumatic brain injury: support for a neuroprotective role of iNOS. J. Cereb. Blood Flow Metab. 25, 673–684.

Bazarian, J.J., Zemlan, F.P., Mookerjee, S., and Stigbrand T. (2006). Serum S-100B and cleaved-tau are poor predictors of long-term outcome after mild traumatic brain injury. Brain Inj. 20, 759–765.

Beer, R., Franz, G., Srinivasan, A., Hayes, R.L., Pike, B.R., Newcomb, J.K., Zhao, X., Schmutzhard, E., Poewe, W., and Kampfl, A. (2000). Temporal profile and cell subtype distribution of activated caspase-3 following experimental traumatic brain injury. J. Neurochem. 75, 1264–1273.

Belanger, H.G., Scott, S.G., Scholten, J., Curtiss, G., and Vanderploeg, R.D. (2005). Utility of mechanism-of-injury-based assessment and treatment: Blast Injury Program case illustration. J. Rehabil. Res. Dev. 42, 403–412.

Berger, R.P., Adelson, P.D., Pierce, M.C., Dulani, T., Cassidy, L.D., and Kochanek, P.M. (2005). Serum neuron-specific enolase, S100B, and myelin basic protein concentrations after inflicted and noninflicted traumatic brain injury in children. J. Neurosurg. 103(1 Suppl), 61–68.

Berger, R.P., Beers, S.R., Richichi, R., Wiesman, D., and Adelson, P.D. (2007). Serum biomarker concentrations and outcome after pediatric traumatic brain injury. J. Neurotrauma. 24, 1793–1801.

Berger, R.P., Dulani, T., Adelson, P.D., Leventhal, J.M., Richichi, R., and Kochanek, P.M. (2006). Identification of inflicted traumatic brain injury in well-appearing infants using serum and cerebrospinal markers: a possible screening tool. Pediatrics 117, 325–332.

Bhattacharjee, Y. (2008). Neuroscience. Shell shock revisited: solving the puzzle of blast trauma. Science 319, 406–408.

Biomarkers Definitions Working Group. (2001). Biomarkers and surrogate endpoints: preferred definitions and conceptual framework. Clin. Pharmacol. Ther. 69, 89–95.

Cernak, I., Ignjatovic, D., Andelic, G., and Savic, J. (1991a). [Metabolic changes as part of the general response of the body to the effect of blast waves]. Vojnosanit. Pregl. 48, 515–522.

Cernak, I., Radosevic, P., Malicevic, Z., and Savic, J. (1995). Experimental magnesium depletion in adult rabbits caused by blast overpressure. Magnes. Res. 8, 249–259.

Cernak, I., Savic, J., Ignjatovic, D., and Jevtic, M. (1999a). Blast injury from explosive munitions. J. Trauma 47, 96–103; discussion 103–104.

Cernak, I., Savic, J., Mrsulja, B., and Duricic, B. (1991b). [Pathogenesis of pulmonary edema caused by blast waves]. Vojnosanit. Pregl. 48, 507–514.

Cernak, I., Savic, J., Zunic, G., Pejnovic, N., Jovanikic, O., and Stepic, V. (1999b). Recognizing, scoring, and predicting blast injuries. World J. Surg. 23, 44–53.

Cernak, I., Savic, V.J., Lazarov, A., Joksimovic, M., and Markovic, S. (1999c). Neuroendocrine responses following graded traumatic brain injury in male adults. Brain Inj. 13, 1005–1015.

Cernak, I., Wang, Z., Jiang, J., Bian, X., and Savic, J. (2001a). Cognitive deficits following blast injury-induced neurotrauma: possible involvement of nitric oxide. Brain Inj. 15, 593–612.

Cernak, I., Wang, Z., Jiang, J., Bian, X., and Savic, J. (2001b). Ultrastructural and functional characteristics of blast injury-induced neurotrauma. J. Trauma 50, 695–706.

Chavko, M., Prusaczyk, W.K., and McCarron, R.M. (2006). Lung injury and recovery after exposure to blast overpressure. J. Trauma 61, 933–942.

Chung, C.W., Song, Y.H., Kim, I.K., Yoon, W.J., Ryu, B.R., Jo, D.G., Woo, H.N., Kwon, Y.K., Kim, H.H., Gwag, B.J., Mook-Jung, I.H., and Jung, Y.K. (2001). Proapoptotic effects of tau cleavage product generated by caspase-3. Neurobiol. Dis. 8, 162–172.

Cramer, F., Paster, S., and Stephenson, C. (1949). Cerebral injuries due to explosion waves, cerebral blast concussion; a pathologic, clinical and electroencephalographic study. Arch. Neurol. Psychiatry 61, 1–20.

Dambinova, S.A., Khounteev, G.A., Izykenova, G.A., Zavolokov, I.G., Ilyukhina, A.Y., and Skoromets, A.A. (2003). Blood test detecting autoantibodies to N-methyl-D-aspartate neuroreceptors for evaluation of patients with transient ischemic attack and stroke. Clin. Chem. 49, 1752–1762.

Elsayed, N.M. (1997). Toxicology of blast overpressure. Toxicology 121, 1–15.

Elsayed, N.M., and Gorbunov, N.V. (2003). Interplay between high energy impulse noise (blast) and antioxidants in the lung. Toxicology 189, 63–74.

Elsayed, N.M., and Gorbunov, N.V. (2007). Pulmonary biochemical and histological alterations after repeated low-level blast overpressure exposures. Toxicol. Sci. 95, 289–296.

Elsayed, N.M., Gorbunov, N.V., and Kagan, V.E. (1997). A proposed biochemical mechanism involving hemoglobin for blast overpressure-induced injury. Toxicology 121, 81–90.

Elsayed, N.M., Tyurina, Y.Y., Tyurin, V.A., Menshikova, E.V., Kisin, E.R., Kagan, V.E. (1996). Antioxidant depletion, lipid peroxidation, and impairment of calcium transport induced by air-blast overpressure in rat lungs. Exp. Lung Res. 22, 179–200.

Foley, L.M., Hitchens, T.K., Melick, J.A., Bayir, H., Ho, C., and Kochanek, P.M. (2008). Effect of inducible nitric oxide synthase on cerebral blood flow after experimental traumatic brain injury in mice. J. Neurotrauma 25, 299–310.

Gabbita, S.P., Scheff, S.W., Menard, R.M., Roberts, K., Fugaccia, I., and Zemlan, F.P. (2005). Cleaved-tau: a biomarker of neuronal damage after traumatic brain injury. J. Neurotrauma 22, 83–94.

Galea, E., Dupouey, P., and Feinstein, D.L. (1995). Glial fibrillary acidic protein mRNA isotypes: expression *in vitro* and *in vivo*. J. Neurosci. Res. 41, 452–461.

Gorbunov, N.V., Elsayed, N.M., Kisin, E.R., Kozlov, A.V., and Kagan, V.E. (1997). Air blast-induced pulmonary oxidative stress: interplay among hemoglobin, antioxidants, and lipid peroxidation. Am. J. Physiol. 272, L320–L334.

Gorbunov, N.V., Osipov, A.N., Sweetland, M.A., Day, B.W., Elsayed, N.M., Kagan, V.E. (1996). NO-redux paradox: direct oxidation of alpha-tocopheral and alpha-tocopherol mediated oxidation of ascorbate. Biochem. Biophys. Res. Commun. 219, 835–841.

Guy, R.J., Glover, M.A., and Cripps, N.P. (2000a). Primary blast injury: pathophysiology and implications for treatment. Part III: Injury to the central nervous system and the limbs. J. R. Nav. Med. Serv. 86, 27–31.

Guy, R.J., Kirkman, E., Watkins, P.E., and Cooper, G.J. (1998). Physiologic responses to primary blast. J. Trauma 45, 983–987.

Guy, R.J., Watkins, P.E., and Edmondstone, W.M. (2000b). Electrocardiographic changes following primary blast injury to the thorax. J. R. Nav. Med. Serv. 86, 125–133.

Haskins, W.E., Kobeissy, F.H., Wolper, R.A., Ottens, A.K., Kitlen, J.W., McClung, S.H., O'Steen, B.E., Chow, M.M., Pineda, J.A., Denslow, N.D., Hayes, R.L., and Wang, K.K. (2005). Rapid discovery of putative protein biomarkers of traumatic brain injury by SDS-PAGE-capillary liquid chromatography-tandem mass spectrometry. J. Neurotrauma 22, 629–644.

Hayakata, T., Shiozaki, T., Tasaki, O., Ikegawa, H., Inoue, Y., Toshiyuki, F., Hosotubo, H., Kieko, F., Yamashita, T., Tanaka, H., Shimazu, T., and Sugimoto, H. (2004). Changes in CSF S100B and cytokine concentrations in early-phase severe traumatic brain injury. Shock 22, 102–107.

Hoge, C.W., McGurk, D., Thomas, J.L., Cox, A.L., Engel, C.C., and Castro, C.A. (2008). Mild traumatic brain injury in U.S. soldiers returning from Iraq. N. Engl. J. Med. 358, 453–463.

Hurley, R.A., McGowan, J.C., Arfanakis, K., and Taber, K.H. (2004). Traumatic axonal injury: novel insights into evolution and identification. J. Neuropsychiatry Clin. Neurosci. 16, 1–7.

Ingebrigtsen, T., and Romner, B. (2003). Biochemical serum markers for brain damage: a short review with emphasis on clinical utility in mild head injury. Restor. Neurol. Neurosci. 21, 171–176.

Jaffin, J.H., McKinney, L., Kinney, R.C., Cunningham, J.A., Moritz, D.M., Kraimer, J.M., Graeber, G.M., Moe, J.B., Salander, J.M., and Harmon, J.W. (1987). A laboratory model for studying blast overpressure injury. J. Trauma 27, 349–356.

Januszkiewicz, A.J., Mundie, T.G., and Dodd, K.T. (1997). Maximal exercise performance-impairing effects of simulated blast overpressure in sheep. Toxicology 121, 51–63.

Johnsson, P., Blomquist, S., Luhrs, C., Malmkvist, G., Alling, C., Solem, J.O., and Stahl, E. (2000). Neuron-specific enolase increases in plasma during and immediately after extracorporeal circulation. Ann. Thorac. Surg. 69, 750–754.

Kato, K., Fujimura, M., Nakagawa, A., Saito, A., Ohki, T., Takayama, K., and Tominaga, T. (2007). Pressure-dependent effect of shock waves on rat brain: induction of neuronal apoptosis mediated by a caspase-dependent pathway. J. Neurosurg. 106, 667–676.

Kaur, C., Singh, J., Lim, M.K., Ng, B.L., and Ling, E.A. (1997a). Macrophages/microglia as 'sensors' of injury in the pineal gland of rats following a non-penetrative blast. Neurosci. Res. 27, 317–322.

Kaur, C., Singh, J., Lim, M.K., Ng, B.L., Yap, E.P., and Ling, E.A. (1995). The response of neurons and microglia to blast injury in the rat brain. Neuropathol. Appl. Neurobiol. 21, 369–377.

Kaur, C., Singh, J., Lim, M.K., Ng, B.L., Yap, E.P., and Ling, E.A. (1996). Studies of the choroid plexus and its associated epiplexus cells in the lateral ventricles of rats following an exposure to a single non-penetrative blast. Arch. Histol. Cytol. 59, 239–248.

Kaur, C., Singh, J., Lim, M.K., Ng, B.L., Yap, E.P., and Ling, E.A. (1997b). Ultrastructural changes of macroglial cells in the rat brain following an exposure to a non-penetrative blast. Ann. Acad. Med. Singapore 26, 27–29.

Kaur, C., Singh, J., Moochhala, S., Lim, M.K., Lu, J., and Ling, E.A. (1999). Induction of NADPH diaphorase/nitric oxide synthase in the spinal cord motor neurons of rats following a single and multiple non-penetrative blasts. Histol. Histopathol. 14, 417–425.

Kennedy, J.E., Jaffee, M.S., Leskin, G.A., Stokes, J.M., Leal, F.O., and Fitzpatrick, P.J. (2007). Posttraumatic stress disorder and posttraumatic stress disorder-like symptoms and mild traumatic brain injury. J. Rehabil. Res. Dev. 44, 895–920.

King, N.S. (2008). PTSD and traumatic brain injury: folklore and fact? Brain Inj. 22, 1–5.

Kleindienst, A., Hesse, F., Bullock, M.R., and Buchfelder, M. (2007). The neurotrophic protein S100B: value as a marker of brain damage and possible therapeutic implications. Prog. Brain Res. 161, 317–325.

Kleindienst, A., and Ross Bullock, M. (2006). A critical analysis of the role of the neurotrophic protein S100B in acute brain injury. J. Neurotrauma 23, 1185–1200.

Kobeissy, F.H., Ottens, A.K., Zhang, Z., Liu, M.C., Denslow, N.D., Dave, J.R., Tortella, F.C., Hayes, R.L., and Wang, K.K. (2006). Novel differential neuroproteomics analysis of traumatic brain injury in rats. Mol. Cell Proteomics 5, 1887–1898.

Korfias, S., Stranjalis, G., Boviatsis, E., Psachoulia, C., Jullien, G., Gregson, B., Mendelow, A.D., and Sakas, D.E. (2007). Serum S-100B protein monitoring in patients with severe traumatic brain injury. Intensive Care Med. 33, 255–260.

Lescuyer, P., Hochstrasser, D., and Rabilloud, T. (2007). How shall we use the proteomics toolbox for biomarker discovery? J. Proteome Res. 6, 3371–3376.

Lew, H.L. (2005). Rehabilitation needs of an increasing population of patients: Traumatic brain injury, polytrauma, and blast-related injuries. J. Rehabil. Res. Dev. 42, xiii–xvi.

Lew, H.L., Poole, J.H., Alvarez, S., and Moore, W. (2005). Soldiers with occult traumatic brain injury. Am. J. Phys. Med. Rehabil. 84, 393–398.

Lucas, S.M., Rothwell, N.J., and Gibson, R.M. (2006). The role of inflammation in CNS injury and disease. Br. J. Pharmacol. 147(Suppl 1), S232–S240.

Mayorga, M.A. (1997). The pathology of primary blast overpressure injury. Toxicology 121, 17–28.

Michetti, F., and Gazzolo, D. (2002). S100B protein in biological fluids: a tool for perinatal medicine. Clin. Chem. 48, 2097–2104.

Moochhala, S.M., Md, S., Lu, J., Teng, C.H., and Greengrass, C. (2004). Neuroprotective role of aminoguanidine in behavioral changes after blast injury. J. Trauma 56, 393–403.

Murthy, J.M., Chopra, J.S., and Gulati, D.R. (1979). Subdural hematoma in an adult following a blast injury. Case report. J. Neurosurg. 50, 260–261.

Nath, R., Probert, A., Jr., McGinnis, K.M., and Wang, K.K. (1998). Evidence for activation of caspase-3-like protease in excitotoxin- and hypoxia/hypoglycemia-injured neurons. J. Neurochem. 71, 186–195.

Nylen, K., Ost, M., Csajbok, L.Z., Nilsson, I., Blennow, K., Nellgard, B., and Rosengren, L. (2006). Increased serum-GFAP in patients with severe traumatic brain injury is related to outcome. J. Neurol. Sci. 240, 85–91.

Ottens, A.K., Kobeissy, F.H., Golden, E.C., Zhang, Z., Haskins, W.E., Chen, S.S., Hayes, R.L., Wang, K.K., and Denslow, N.D. (2006). Neuroproteomics in neurotrauma. Mass Spectrom. Rev. 25, 380–408.

Park, S.Y., and Ferreira, A. (2005). The generation of a 17 kDa neurotoxic fragment: an alternative mechanism by which tau mediates beta-amyloid-induced neurodegeneration. J. Neurosci. 25, 5365–5375.

Park, S.Y., Tournell, C., Sinjoanu, R.C., and Ferreira, A. (2007). Caspase-3- and calpain-mediated tau cleavage are differentially prevented by estrogen and testosterone in beta-amyloid-treated hippocampal neurons. Neuroscience 144, 119–127.

Pelinka, L.E., Hertz, H., Mauritz, W., Harada, N., Jafarmadar, M., Albrecht, M., Redl, H., and Bahrami, S. (2005). Nonspecific increase of systemic neuron-specific enolase after trauma: clinical and experimental findings. Shock 24, 119–123.

Pelinka, L.E., Kroepfl, A., Leixnering, M., Buchinger, W., Raabe, A., and Redl, H. (2004). GFAP versus S100B in serum after traumatic brain injury: relationship to brain damage and outcome. J. Neurotrauma 21, 1553–1561.

Piazza, O., Storti, M.P., Cotena, S., Stoppa, F., Perrotta, D., Esposito, G., Pirozzi, N., and Tufano, R. (2007). S100B is not a reliable prognostic index in paediatric TBI. Pediatr. Neurosurg. 43, 258–264.

Pike, B.R., Flint, J., Dutta, S., Johnson, E., . Wang, K.K., and Hayes, R.L. (2001). Accumulation of non-erythroid alpha II-spectrin and calpain-cleaved alpha II-spectrin breakdown products in cerebrospinal fluid after traumatic brain injury in rats. J. Neurochem. 78, 1297–1306.

Pike, B.R., Zhao, X., Newcomb, J.K., Posmantur, R.M., Wang, K.K., and Hayes, R.L. (1998a). Regional calpain and caspase-3 proteolysis of alpha-spectrin after traumatic brain injury. Neuroreport 9, 2437–2442.

Pike, B.R., Zhao, X., Newcomb, J.K., Wang, K.K., Posmantur, R.M., and Hayes, R.L. (1998b). Temporal relationships between de novo protein synthesis, calpain and caspase 3-like protease activation, and DNA fragmentation during apoptosis in septo-hippocampal cultures. J. Neurosci. Res. 52, 505–520.

Pineda, J.A., Lewis, S.B., Valadka, A.B., Papa, L., Hannay, H.J., Heaton, S.C., Demery, J.A., Liu, M.C., Aikman, J.M., Akle, V., Brophy, G.M., Tepas, J.J., Wang, K.K., Robertson, C.S., and Hayes, R.L. (2007). Clinical significance of alphaII-spectrin breakdown products in cerebrospinal fluid after severe traumatic brain injury. J. Neurotrauma 24, 354–366.

Pineda, J.A., Wang, K.K., and Hayes, R.L. (2004). Biomarkers of proteolytic damage following traumatic brain injury. Brain Pathol. 14, 202–209.

Ringger, N.C., O'Steen, B.E., Brabham, J.G., Silver, X., Pineda, J., Wang, K.K., Hayes, R.L., and Papa, L. (2004). A novel marker for traumatic brain injury: CSF alphaII-spectrin breakdown product levels. J. Neurotrauma 21, 1443–1456.

Saljo, A., Bao, F., Haglid, K.G., and Hansson, H.A. (2000). Blast exposure causes redistribution of phosphorylated neurofilament subunits in neurons of the adult rat brain. J. Neurotrauma 17, 719–726.

Savic, J., Tatic, V., Ignjatovic, D., Mrda, V., Erdeljan, D., Cernak, I., Vujnov, S., Simovic, M., Andelic, G., and Duknic, M. (1991). [Pathophysiologic reactions in sheep to blast waves from detonation of aerosol explosives]. Vojnosanit. Pregl. 48, 499–506.

Shiozaki, T., Hayakata, T., Tasaki, O., Hosotubo, H., Fuijita, K., Mouri, T., Tajima, G., Kajino, K., Nakae, H., Tanaka, H., Shimazu, T., and Sugimoto, H. (2005). Cerebrospinal fluid concentrations of anti-inflammatory mediators in early-phase severe traumatic brain injury. Shock 23, 406–410.

Stuhmiller, J.H., Ho, K.H., Vander Vorst, M.J., Dodd, K.T., Fitzpatrick, T., and Mayorga, M. (1996). A model of blast overpressure injury to the lung. J. Biomech. 29, 227–234.

Taber, K.H., Warden, D.L., and Hurley, R.A. (2006). Blast-related traumatic brain injury: what is known? J. Neuropsychiatry Clin. Neurosci. 18, 141–145.

Vander Vorst, M., Ono, K., Chan, P., and Stuhmiller, J. (2007). Correlates to traumatic brain injury in nonhuman primates. J. Trauma 62, 199–206.

Vinores, S.A., Herman, M.M., Rubinstein, L.J., and Marangos, P.J. (1984). Electron microscopic localization of neuron-specific enolase in rat and mouse brain. J. Histochem. Cytochem. 32, 1295–1302.

Wang, K.K., Ottens, A.K., Liu, M.C., Lewis, S.B., Meegan, C., Oli, M.W., Tortella, F.C., and Hayes, R.L. (2005). Proteomic identification of biomarkers of traumatic brain injury. Expert Rev. Proteomics 2, 603–614.

Wang, K.K., Posmantur, R., Nath, R., McGinnis, K., Whitton, M., Talanian, R.V., Glantz, S.B., and Morrow, J.S. (1998). Simultaneous degradation of alphaII- and betaII-spectrin by caspase 3 (CPP32) in apoptotic cells. J. Biol. Chem. 273, 22490–22497.

Yilmaz, S., and Pekdemir, M. (2007). An unusual primary blast injury: Traumatic brain injury due to primary blast injury. Am. J. Emerg. Med. 25, 97–98.

Zemlan, F.P., Jauch, E.C., Mulchahey, J.J., Gabbita, S.P., Rosenberg, W.S., Speciale, S.G., and Zuccarello, M. (2002). C-tau biomarker of neuronal damage in severe brain injured patients: association with elevated intracranial pressure and clinical outcome. Brain Res. 947, 131–139.

Zhang, C., Siman, R., Xu, Y.A., Mills, A.M., Frederick, J.R., and Neumar, R.W. (2002). Comparison of calpain and caspase activities in the adult rat brain after transient forebrain ischemia. Neurobiol. Dis. 10, 289–205.

Address reprint requests to:
Stanislav I. Svetlov, M.D., Ph.D.
Senior Principal Scientist
Center of Innovative Research
Banyan Biomarkers, Inc.
12085 Research Drive
Alachua, FL 32615

E-mail: ssvetlov@banyanbio.com

Morphologic and Biochemical Characterization of Brain Injury in a Model of Controlled Blast Overpressure Exposure

Stanislav I. Svetlov, MD, PhD, Victor Prima, PhD, Daniel R. Kirk, PhD, Hector Gutierrez, PhD, Kenneth C. Curley, MD, Ronald L. Hayes, PhD, and Kevin K. W. Wang, PhD

Objectives: Existing experimental approaches for studies of blast impact in small animals are insufficient and lacking consistency. Here, we present a comprehensive model, with repeatable blast signatures of controlled duration, peak pressure, and transmitted impulse, accurately reproducing blast impact in laboratory animals.

Materials: Rat survival, brain pathomorphology, and levels of putative biomarkers of brain injury glial fibrillary acid protein (GFAP), neuron-specific enolase, and ubiquitin C-terminal hydrolase (UCH)-L1 were examined in brain, cerebrospinal fluid (CSF), and blood after 10 msec of 358 kPa peak overpressure blast exposure.

Results: The high-speed imaging demonstrated a strong head acceleration/jolting accompanied by typical intracranial hematomas and brain swelling. Microscopic injury was revealed by prominent silver staining in deep brain areas, including the nucleus subthalamicus zone, suggesting both diffused and focal neurodegeneration. GFAP and 2′,3′-cyclic nucleotide 3′-phosphodiesterase (CNPase), markers of astroglia and oligodendroglia, accumulated substantially in the hippocampus 24 hours after blast and persisted for 30 days postblast. However, GFAP content in the blood significantly increased 24 hours after injury, followed by a decline and subsequent accumulation in CSF in a time-dependent fashion. A similar profile is shown for UCH-L1 increase in blood, whereas increased CSF levels of UCH-L1 persisted throughout 14 days after blast and varied significantly in individual rats. Neuron-specific enolase levels in blood were significantly elevated within 24 hours and 48 hours postblast.

Conclusions: The proposed model of controlled nonpenetrating blast in rats demonstrates the critical pathologic and biochemical signatures of blast brain injury that may be triggered by cerebrovascular responses, including blood-brain barrier disruption, glia responses, and neuroglial alterations.

Key Words: Blast, Brain injury, Experimental models, Biomarkers, UCH-L1, GFAP, CNPase.

(*J Trauma.* 2010;69: 795–804)

Submitted for publication May 8, 2009.
Accepted for publication July 23, 2009.

From the Center of Innovative Research (S.I.S., V.P., R.L.H., K.K.W.W.), Banyan Biomarkers, Inc, Alachua, Florida; Department of Mechanical and Aerospace Engineering (D.R.K., H.G.), Florida Institute of Technology, Melbourne, Florida; Departments of Physiological Sciences (S.I.S.) and Psychiatry (K.K.W.W.), University of Florida, Gainesville, Florida; and U.S. Army Medical Research and Materiel Command (MRMC) (K.C.C.), Fort Detrick, Frederick, Maryland.
Supported by Department of Defense grants N14-06-1-1029, W81XWH-8-1-0376, and W81XWH-07-01-0701.
The views expressed herein are those of the authors and do not reflect the official policy or position of the Department of the Army, Department of Defense, or the U.S. government.
Address for reprints: Stanislav I. Svetlov, MD, PhD, Center of Innovative Research, Banyan Biomarkers, Inc, 12085 Research Drive, Alachua, FL 32615; email: ssvetlov@banyanbio.com.

DOI: 10.1097/TA.0b013e3181bbd885

Several decades of medical literature, and particularly recent military operations, provide a number of cases in which brain injuries are likely to have resulted from primary blast forces.[1,2] Thus, identifying pathogenic pathways of primary blast brain injury (BBI) in reproducible experimental models is vital to the development of diagnostic algorithms for mild traumatic brain injury (TBI) through severe TBI, and eventually differentiating mild TBI from posttraumatic stress disorder. A number of experimental animal models, which include rodents and larger animals such as sheep, have been implemented to study the mechanisms of blast wave impacts.[3,4] However, because of inconsistent designs among blast generators used in the different studies, the data on brain injury mechanisms and putative biomarkers have been difficult to analyze and compare.[5–9]

Although there are currently no biomarkers with proven clinical utility for the diagnostics of TBI, whether caused by blast, mechanical trauma, stroke, or other acute brain injuries, research has uncovered several valuable candidates that have shown preclinical and clinical potential.[10] The ones currently generating the most interest include neuron-specific enolase (NSE), glial fibrillary acid protein (GFAP), S-100ß, and myelin basic protein. Although these proteins are still being assessed, they appear to lack either the necessary sensitivity or the brain specificity (except perhaps GFAP) to be used effectively alone.[11,12] However, the combination of these markers can effectively detect conventional TBI and provide outcome predictions.[13,14]

For studies of mechanisms and biomarkers of BBI, we developed and used a model of "composite" blast exposure with controlled parameters of blast wave exposure and brain injury in rats. In this article, we demonstrate that brain damage induced by severe head-directed blast waves is accompanied by time-dependent intracranial hemorrhages and neurodegeneration in deep areas of the brain. This was accompanied by the accumulation of GFAP, NSE, and ubiquitin C-terminal hydrolase (UCH)-L1 in blood and cerebrospinal fluid (CSF) with a characteristic time course suggestive of a rapid blood-brain barrier disruption following blast exposure.

MATERIALS AND METHODS

Shock Tube Design, Construction, and Setup

A compressed air-driven shock tube was used to expose rats to a supra-atmospheric wave of air pressure. A shock tube capable of generating a wide range of controlled blast

waves without the use of explosives was designed, constructed, and tested at both the Florida Institute of Technology and Banyan Biomarkers, Inc. (Fig. 1, A). The tube is separated into two sections, high pressure (driver) and low pressure (driven), separated by a metal diaphragm. The thickness, type of material, driver/driven ratio, and initial driver pressure determine the peak and duration of the overpressure (OP) event. In the presented series of experiments, 0.05-mm thick stainless steel diaphragms were used to generate high-pressure shock waves. The ratio of driver versus driven section lengths was 15 to 1. The driver section was initialized to a pressure of 5,170 kPa and the driven section was left at ambient pressure. The diaphragm rupture initiated by an internal cutter leads to the sudden exposure of a low-pressure air to gas at significantly higher pressure, resulting in the formation of a shock wave. The blast pressure data were acquired using piezoelectric blast pressure transducers and LabView 8.2 software. A National Instruments 1.25 Msamples/sec data acquisition card was used to acquire data from multiple channels. The shock tube was calibrated, so that the peak OP indicated the actual measures (kPa) at the surface of the rat's skull. Images of the rat head during the blast event were captured at 1,000 frames/sec using a high-speed video camera and Schlieren optics.

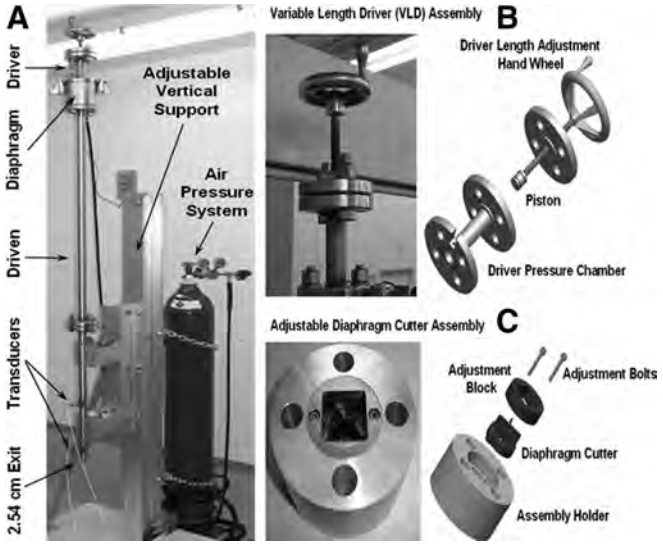

Figure 1. Blast generator setup. Overview of the shock tube (*A*), variable length driver (VLD) assembly (*B*), and adjustable diaphragm cutter unit (*C*), see Materials and Methods section for detail.

Animal Exposure to a Controlled Blast Wave

All rats were anesthetized with isoflurane inhalations described previously in detail. After reaching a deep plane of anesthesia, they were placed into a holder exposing only their head (body-armored setup) at the distance 5 cm from the exit nozzle of the shock tube, which was perpendicular to the middle of the head (Fig. 2). The head laid on a flexible mesh surface composed of a thin steel grating. This diminished the surface reflection of blast waves and decreased the formation of secondary waves that would potentially exacerbate the injury. For pathomorphology and biomarker studies, animals were then subjected to a single blast wave with a mean peak

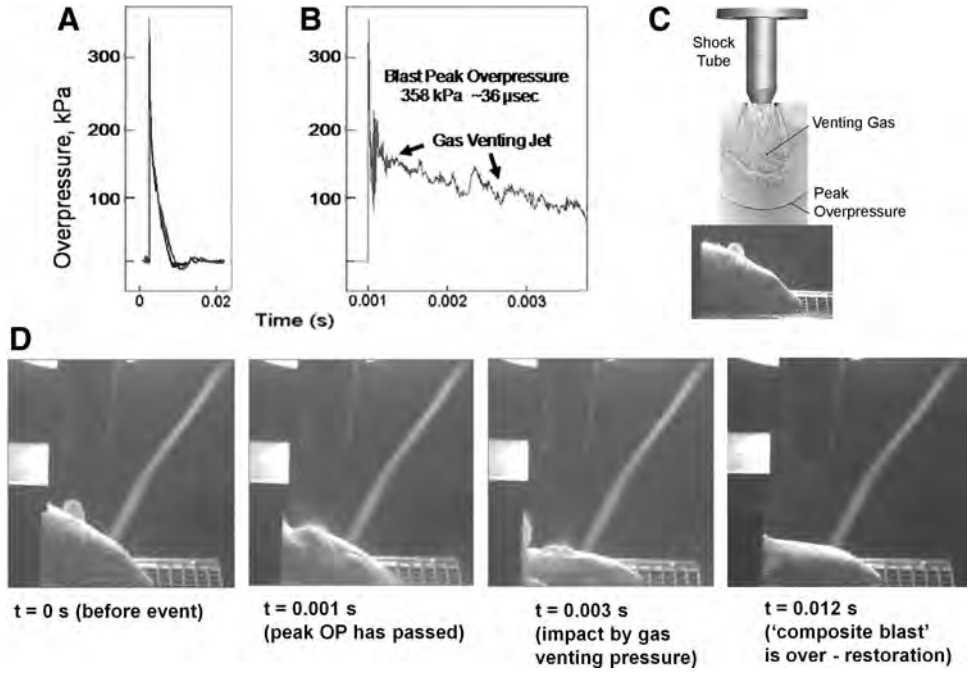

Figure 2. Experimental outline. (*A*) General shape of blast wave hitting an experimental animal showing a presence of negative phase; (*B*) components of shock tube-generated blast wave; (*C*) specimen positioning relative to shock tube, and (*D*) rat head movement and deformation after head-directed, body armored, blast wave exposure of 358 kPa for 10 msec 1,000 Hz high-speed video images using Schlieren optics shown.

TABLE 1. Rat Mortality After Exposure of Total Body and Head (Body Armored) to "Composite Blast"

Peak Overpressure (kPa)	Total Blast Duration (msec)	Mortality
Total exposure (unprotected body)		
110 (n = 3)	2	Survived
170 (n = 2)	4	Lethal
358 (n = 2)	1	Lethal
Head directed (body armored)		
172 (n = 12)	4	All survived
358 (n = 48)	10	All but one survived

Anesthetized rats were placed on a platform in dorsal-up recumbence at different distances from the nozzle. Rats were subjected to blast wave exposures of various magnitude and duration that included exposure to peak overpressure plus gas venting. The magnitude and duration of blast were assessed using data acquired with dynamic blast pressure transducers (see Materials and Methods section for details).

OP of 358 kPa at the head and a total positive-pressure phase duration of ~10 msec (Fig. 2). Because a total blast of 358 kPa magnitude/10 msec duration produced a very strong effect (Fig. 2), although being nonlethal (Table 1), these parameters were chosen for the initial pathomorphology/biomarker assessment presented in this study. For survival studies, body-armored rats were also exposed to head-directed blast of 172 kPa for a total duration of 4 msec. In addition, survival/mortality was investigated in rats exposed to head-directed blast of different magnitude/duration without body protection as shown in Table 1. Two control groups of animals, sham and naïve, underwent the same treatment (anesthesia, handling, and recovery) except they were not exposed to blast. The rats in a sham group were exposed to the noise of a single blast at the 2 m from the shock tube while anesthetized.

Fresh Tissues Collection

At the required time points after blast exposure, animals were killed according to the guidelines approved by the Institutional Animal Care and Use Committee (IACUC) of the University of Florida and tissue samples were collected, snap frozen, and stored at -70°C until further analysis. The rats were anesthetized with 3% to 5% isoflurane in a carrier gas of oxygen using an induction chamber. At the loss of toe pinch reflex, the anesthetic flow was reduced to 1% to 3% and rat was secured in a stereotaxic frame with its head allowed to move freely along the longitudinal axis. A nose cone continued to deliver the anesthetic gases. A dorsal midline incision was made over the cervical vertebrae and occiput. The atlanto-occipital membrane was exposed by blunt dissection. CSF was collected by lowering a 25-gauge needle attached to polyethylene tubing into the cisterna magna. Immediately after CSF collection, the rat was turned over. The chest cavity was opened and 3 mL to 6 mL of blood was withdrawn directly from the heart. After blood collection, the animal was removed from the stereotaxic frame and immediately decapitated (while still under the effects of the anesthesia gases) for fresh brain tissue collection.

Histologic Processing and Staining

Neurodegeneration in injured brains was examined by the de Olmos amino cupric silver histochemical technique developed to study the disintegrative degeneration as previously described in detail.[15,16] At the intended time of sacrifice, rats were deeply anesthetized with sodium pentobarbital (100 mg/kg I.P.) and transcardially perfused with 0.8% NaCl, 0.4% dextrose, 0.8% sucrose, 0.023% $CaCl_2$, and 0.034% sodium cacodylate, followed by a fixative solution containing 4% paraformaldehyde, 4% sucrose, and 1.4% sodium cacodylate. After decapitation, the heads were stored in the perfusion fix for 14 hours, after which the brains were removed, placed in cacodylate storage buffer, and processed for histologic analyses (Neuroscience Associates, Knoxville, TN). Frozen 35-μm-thick coronal sections, taken 420 μm apart between 1.1 mm anterior and 4.4 mm posterior to bregma, were silver stained for neuronal degeneration and counter stained with neutral red. The brain sections were scanned at high resolution.

Western Blot Analysis of Cortex and Hippocampus With GFAP and CNPase

For Western blot analyses, brain tissue samples were homogenized on ice in Western blot buffer as described previously in detail.[17] Samples were subjected to sodium dodecyl sulfate-polyacrylamide gel electrophoresis and electroblotted onto polyvinylidene difluoride membranes. Membranes were blocked in 10 mmol/L Tris, pH 7.5, 100 mmol/L NaCl, and 0.1% Tween-20 containing 5% nonfat dry milk for 60 minutes at room temperature. After overnight incubation with primary antibodies (1:2,000), proteins were detected using a goat anti-rabbit antibody conjugated to alkaline phosphatase (1:10,000–15,000), followed by colorimetric detection system. Bands of interests were normalized for β-actin expression used as a loading control.

GFAP, NSE, and UCH-L1 Enzyme-Linked Immunosorbent Assays

Quantitative detection of UCH-L1 in CSF and plasma was performed using proprietary SW enzyme-linked immunosorbent assay (ELISA) (Banyan Biomarkers, Inc) and recombinant UCH-L1 as standard. For quantification of GFAP and NSE, sandwich ELISA kits from BioVendor (Candler, NC) were used according to the manufacturer's instructions.

Statistics

Statistical analyses were performed using GraphPad Prism 5 software. Values are means ± SEM. Data were evaluated by two-tailed unpaired *t* test and one-way analysis of variance with Dunnett posttest analysis.

RESULTS

Blast Wave Characteristics

To study the injury mechanisms and relevant biomarkers of BBI, the characteristic parameters of the blast waves generated by the shock tube were first considered. The shock tube (Fig. 1) was designed and built to model a freely expanding blast wave as generated by a typical explosion.

Preliminary tests were conducted with no animal specimens to optimize the peak OP and exposure time to accurately reproduce blast events: driver pressure and volume, diaphragm material, and shock tube exit geometry. After the diaphragm rupture, the driver gas sets up a series of pressure waves in the low-pressure driven section that coalesced to form the incident shockwave (Fig. 2, A and B). Both static and dynamic (total) pressures were measured using piezoelectric blast pressure sensors/transducers positioned at the target. The shock wave recorded by blast pressure transducers in the driven section and at the target showed three distinct events: (i) peak OP, (ii) gas venting jet, and (iii) negative-pressure phase. Peak OP, positive phase duration, and impulse appear to be the key parameters that correlate to injury and likelihood of fatality in animals and humans, for various orientations of the specimen relative to the blast wave.[5,18–20] A schematic of a shock tube nozzle and the rat location relative to the shock tube axis, blast OP wave, and gas venting cone is shown in Figure 2, C.

Effect of "Composite Blast" on Rats after Total Body and Head-Directed Exposure

We conducted experiments to compare rat survival upon blast exposure of uncovered versus armored body. The shock tube's nozzle was directed to the rat's head positioned at 5 cm from the opening, along the tube's axis. After exposure of anesthetized rats with unprotected body to blast of 110 kPa (total peak OP) for 2 msec of composite blast wave, all rats remained alive during 24 hours to 48 hours postblast (Table 1). Rats exhibited transitory symptoms of agitation within 15 minutes to 30 minutes after exposure during recovery from anesthesia (data not shown). Further increase of blast OP magnitude to 170 kPa or 358 kPa for total blast duration of 4 msec and 1 msec, respectively, resulted in the increase of rat mortality immediately after blast exposure (Table 1). In contrast, protecting the body significantly increased threshold of mortality, and all rats remained alive after severe blast of 358 kPa peak OP and total duration of ~10 msec (Table 1). Figure 2, D depicts rat head movement and deformation recorded by a high-speed video on this severe head-directed blast wave exposure for 10 msec. Because of the complex nature of the blast event, the brain injury is a result of a combined impact of the "composite" blast including all three major phases of a shock wave shown in Figure 2, A and B. Gas venting jet, albeit lower in magnitude, lasts the longest, represents the bulk of blast impulse and possibly produces the most devastating impact. Figure 2, D demonstrates a strong downward head acceleration after the passage of peak OP that lasts ~36 μsec. However, cranial deformation is more severe during the gas venting phase, lasting up to ~10 msec. Only when the positive-pressure phase is over, the shape of the rat's skull starts to restore. These findings point to a potential flaw in several previous studies described in the literature: animal specimens are usually placed along the axis of the shock wave generator. In such location, the venting gas jet creates a much larger impulse (energy transfer) in the specimen than the peak OP itself. This effect can be virtually eliminated by placing the specimens off-axis from the venting jet in a way that the main effect acting on the specimen is the peak OP event, as will be presented in the Discussion section.

Brain Pathomorphology and Histology

Head acceleration and deformation after severe blast exposure shown in Figure 2 were accompanied by typical focal and massive intracranial hematomas and brain swelling (Fig. 3, B1 and C1). The hemorrhages and hematomas developed within hours after impact and appeared visibly through the undamaged scull at 24 hours to 48 hours after blast exposure (data not shown). The size of hematomas varied significantly in different rats and formed a capsule at 5 days postblast as shown in one the most damaged rat brain after in situ perfusion (Fig. 3, C1). The intracranial blood accumulation partially resolved at day 14 in a majority of rats observed (data not shown). As mentioned earlier, all rats but one remained alive during 14 days of postblast observation. Coronal sections of brains fixed in situ by transcardial perfusion were stained for neurodegeneration using silver impregnation. On microscopic examination, brain sections revealed a prominent silver staining becoming evident in the deep brain areas such as caudal diencephalon, including nucleus subthalamicus zone, at 48 hours postblast (Fig. 3, B2 and C2). The patterns of staining throughout the brain indicate both diffused and focal mild neurodegeneration, predominantly in the deep areas of rostral and caudal diencephalon (Fig. 3, B and C) and mesencephalon (data not shown). Particularly, brain histochemistry indicated a prominent silver accumulation in perivascular spaces and subventricular zones at 48 hours and predominant tissue localization 5 days postblast (Fig. 3, B3 and C3).

Expression of GFAP and CNPase in Brain Cortex and Hippocampus After Blast Impact

There was no significant increase of GFAP in the rat cortex after severe direct blast exposure (Fig. 4, A), in contrast to a significant GFAP accumulation in the hippocampus (Fig. 4, B). It appears to be that GFAP peaked in the hippocampus at 7 days after injury and persisted up to 30 days postblast (Fig. 4, B). In contrast, 2′,3′-cyclic nucleotide 3′-phosphodiesterase (CNPase) accumulated significantly in the cortex between 7 days and 30 days postblast (Fig. 5, A). However, the most prominent, severalfold increase in CNPase expression was found in the hippocampus showing the maximal nearly fourfold increase at 30 days after blast exposure (Fig. 5, B).

We determined quantitatively the amount of GFAP in blood and CSF by commercial sandwich ELISA (SW ELISA) assay. It has been found that increase of GFAP expression in the brain (hippocampus) was accompanied by its rapid and statistically significant accumulation in serum 24 hours after injury followed by a decline thereafter (Fig. 6, A). Although an accumulation of GFAP in CSF was delayed and occurred more gradually, in a time-dependent fashion (Fig. 6, B).

Because GFAP has been considered as a marker of activated astrocytes, the glial activation (gliosis) appears to be a prominent and an early stage feature of blast-induced brain damage.

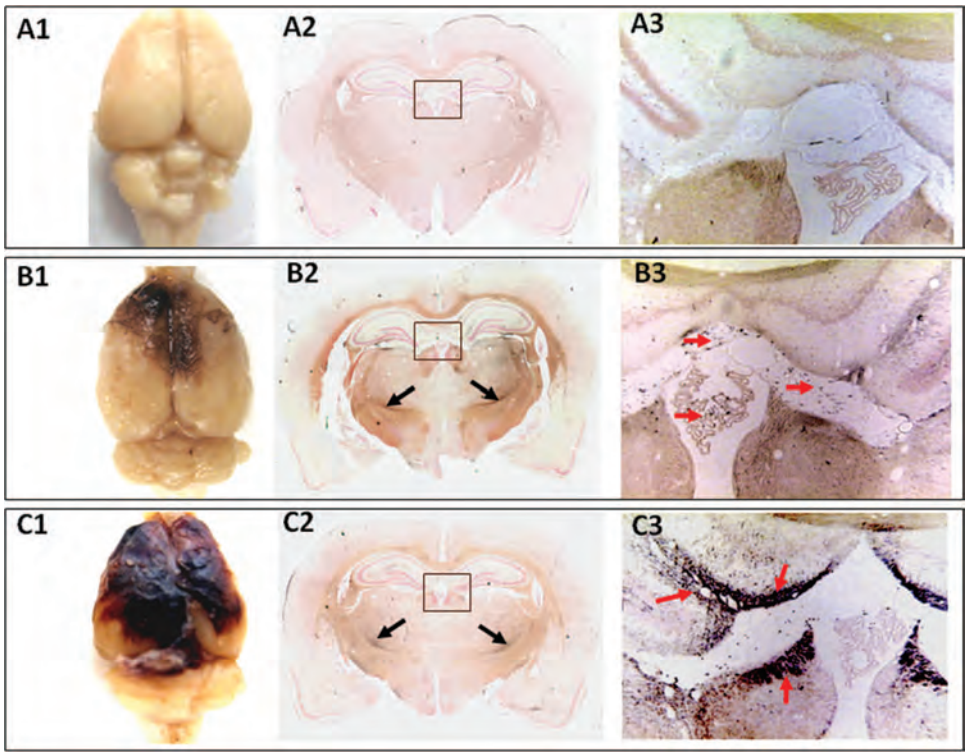

Figure 3. Brain pathomorphology after head-directed exposure to blast wave. Anesthetized rats were subjected to head-directed blast exposure (*B* and *C*) or noise (sham) (*A*). Forty-eight hours after exposures (*A* and *B*) or at 5 days postblast (*C*), brains were perfused in situ, removed, and processed as described in Materials and Methods section in detail. Gross pathology: typical focal intracranial hematomas (*B1* and *C1*) shown from at least three animals at each time point. Histopathology: coronal sections in caudal diencephalon exhibit diffuse and local silver accumulation (*B2* and *C2*). Black arrows indicate strong silver staining in nucleus subthalamicus. Representative microphotographs of whole brains with high-resolution scan (1.5×, *A2–C2*) and corresponding or similar areas at higher magnification (10×) are shown (*A3–C3*). Red arrows point to silver accumulation in perivascular and periventricular tissue zone.

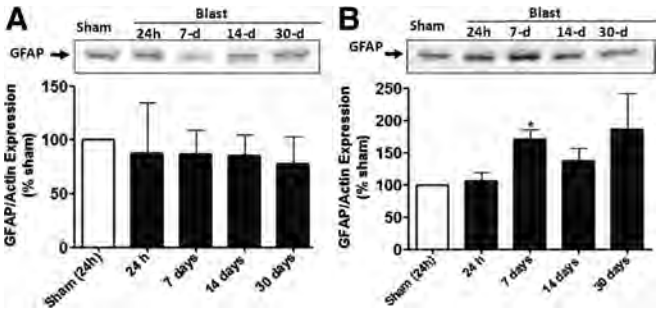

Figure 4. Western blot analysis of GFAP expression in the cortex (*A*) and hippocampus (*B*) of rats with blast-induced nonpenetrating injury. The brains were collected at various times after blast exposure, brain proteins (20 μg) were resolved by SDS-PAGE and immunoblotted with GFAP as described in Materials and Methods section. S, sham (blast noise-treated rats); I, blast wave-exposed rats. Data shown are mean ± SEM of at least three independent experiments. A representative blot out of at least three is shown (*$p < 0.05$).

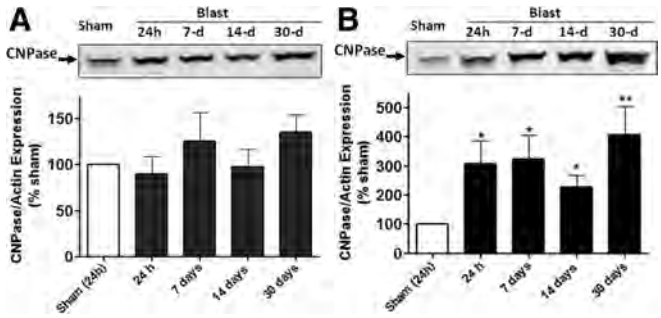

Figure 5. Western blot analysis of CNPase expression in the cortex (*A*) and hippocampus (*B*) of rats with blast-induced nonpenetrating injury. The brains were collected at various times after blast exposure, brain proteins (20 μg) were resolved by SDS-PAGE and immunoblotted with CNPase as described in Materials and Methods section. S, sham (blast noise-treated rats); I, blast wave-exposed rats. Data shown are mean ± SEM of at least three independent experiments. A representative blot out of at least three is shown. (*$p < 0.05$).

NSE and UCH-L1 Accumulation in CSF and Blood After Blast Exposure in Rats

NSE concentrations in serum were determined by commercial SW ELISA assay and were significantly higher at 24 hours and 48 hours postblast period in exposed rats compared with naïve control animals (Fig. 7, B). Although an average of NSE amounts in CSF was substantially high at 24 hours, the difference in CSF levels of NSE

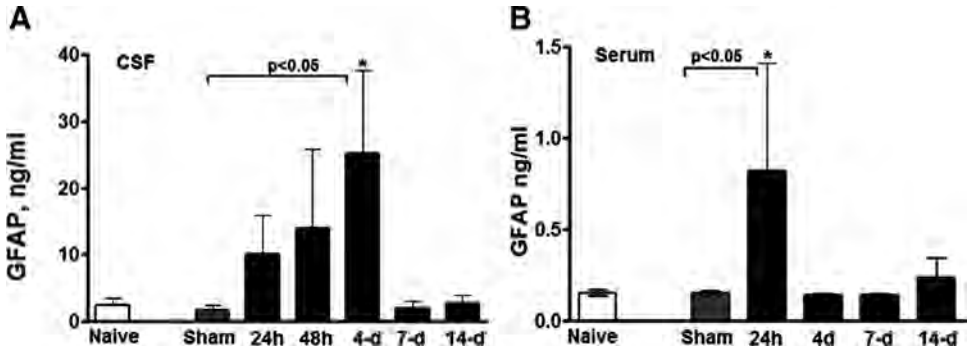

Figure 6. CSF and blood accumulation of GFAP in rats after blast exposure. Rats were subjected to head-directed blast of 358 kPa for total 10 msec. CSF and blood were collected at different times after blast. The levels of GFAP in CSF (*A*) and plasma (*B*) were assayed by SW ELISA as described in Materials and Methods section. Statistical significance was validated using unpaired *t* test and one-way ANOVA with Dunnett posttest analysis. Data shown are mean ± SEM of at least three independent experiments (n = 3–5) (*$p < 0.05$).

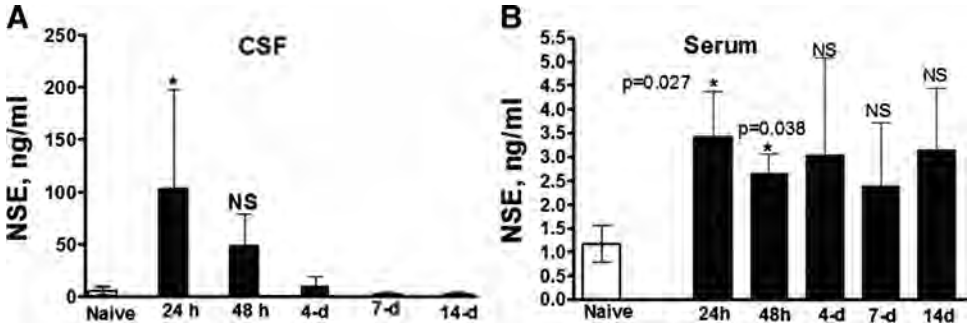

Figure 7. The levels of neurone-specific enolase (NSE) in CSF and blood in rats after blast exposure. Rats were hit by a head-directed blast wave of 358 kPa for total 10 msec. CSF and blood were collected at different times after blast. The levels of NSE in CSF (*A*) and serum (*B*) were assayed by NSE SW ELISA. Unpaired *t* test was used to analyze statistical significance of values. Data shown are mean ± SEM of at least three independent experiments (n = 3–5). (*$p < 0.05$); NS, not significant.

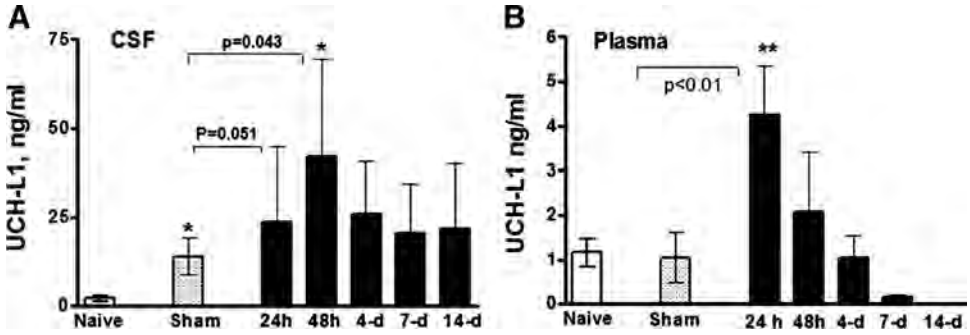

Figure 8. Accumulation of UCH-L1 in CSF and blood in rats after blast exposure. Rats were subjected to a head-directed blast wave of 358 kPa for total 10 msec. CSF and blood were collected at different times postblast. The levels of UCH-L1 in CSF (*A*) and plasma (*B*) were assayed by Banyan UCH-L1 SW ELISA. Unpaired *t* test was used to analyze statistical significance of values. Data shown are mean ± SEM of at least 3 to 10 independent experimental samples of CSF and 4 to 8 experimental samples of plasma (*$p < 0.05$; **$p < 0.01$).

after blast was not statistically significant ($p > 0.05$) and varied remarkably in individual rats that was reflected by the SD values (Fig. 7, A).

To assess UCH-L1 concentration in CSF and blood, we developed validated and used proprietary SW ELISA kit. UCH-L1 rapidly accumulated in blood 24 hours after blast exposure followed by a gradual decline at 14 days postblast recovery period (Fig. 8, B). Average CSF levels of UCH-L1 were slightly increased throughout 14 days after blast exposure and, similarly to NSE and GFAP, varied significantly in individual rats (Fig. 8, A). Both NSE and UCH-L1 have been expressed primarily, but not exclusively, in CNS, localize specifically to the neuronal body and overexpressed during neuronal damage and degeneration.[21–23]

A rapid accumulation of GFAP, NSE, and UCH-L1 in circulation together with a delayed appearance in CSF suggests that cerebrovascular damage, particularly the disruption of blood-brain barrier is a critical and first-response reaction on blast wave exposure.

DISCUSSION

It is still controversial whether primary blast forces directly damage the brain and, if they do, what are the mechanisms mediating the injury[24]? Analysis of mechanisms and development of biomarkers of BBI is complicated by a deficiency of quality experimental studies. Blast generators (shock tubes) are increasingly being used at places such as Walter Reed Army Institute of Research and the Navy Research Laboratory for conducting blast trauma studies on simulated human targets. However, because of inconsistent designs among shock tubes used in the different studies, the data on injury mechanisms, including brain damage, are difficult to analyze and compare if the shock waves used for the experiments are not properly characterized.[5,6,19] A common drawback found in many shock tube blast studies comes from placing the target along the axis of the shock wave generator.[5] This creates exposure to a gas venting jet: after the shock wave passes, the exhaust of the gas used to create the wave substantially alters the pressure and impulse at the target as it vents (Fig. 2, B–D).

The modular design of our shock tube provides the flexibility to perform repeatable blast experiments over a wide range of peak OP, pulse duration, and transferred mechanical energy (impulse), in a relatively lightweight package. A crucial part in using a shock tube for animal blast experiments is reproducibility of the blast events between tests. In our shock tube, the burst pressure of the diaphragm separating the driver and driven sections do not change (Fig. 1). Repeatability of diaphragm burst pressure was accomplished through the use of a cutter assembly directly in front of the diaphragm.[25] Special consideration is also given to properly shaping the exit of the driven section. This is necessary because the structure and flow field of the blast wave at the exit of the tube are influenced by the exit geometry of the driven section. To prevent unnecessary disturbances in the flow field from hindering replication of the proper pressure history at a target, it has been found that the exit of the driven section must be tapered. This allows the blast wave to propagate freely around the end of the driven section without reflecting.

Another important aspect during blast experiments with a shock tube is to ensure proper measurement of the blast event parameters, particularly at the surface of the specimen. To minimize the interaction between the pressure transducer and the target, caused by the alteration in flow pattern in the vicinity of the sensor, the data are first captured at the desired location without any target. After the pressure history is recorded and the sensors removed, the animal can be carefully positioned at the same location and the test repeated because it has been previously demonstrated that the proposed shock tube design has excellent repeatability characteristics.

In the present series of experiments, we placed rats along the shock tube axis (on-axis) and studied the combined effect of blast peak OP and venting gas that creates the impact we call "composite" blast. Although the blast generated in our model is a single blast event, the type of blast load observed resembles the complex effect produced by multiple blasts, such as in a confined space where the blast waves reverberate and overlap, hence the effect of displaced air mass flow on the resultant wave structure and magnitude can be important. It should be noted that in any blast produced in laboratory models, only a particular component of a complex blast experienced on the battlefield is present. We propose that because of the large spherical shape of the blast wave at the exit of the shock tube compared with the confined conical shape of the venting gas (Fig. 2, C), placing a rat outside the gas cone avoids gas venting thus subjecting rats to the effects of a "pure" blast OP. The shock tube was calibrated to achieve desired peak OPs depending on the angle and distance from the tube's nozzle (data not shown). The comparative studies of effects of this pure peak OP component on pathophysiology and biomarkers depending on the magnitude, duration, and number of exposures are under way in our laboratories.

A number of investigations have used compressed air-driven shock tubes and nitrogen-driven blast wave generator[5] for blast exposures of various animals (e.g., rats, mice, and rabbits) to address mechanisms of injury. Small animals are placed in orthopedic stockinette slings and large animals in open mesh nylon TM slings and subjected to blast exposure at varying distances and body orientations with or without a supportive/reflective plate behind the animal (see Ref. 19 for details). A majority of blast injury-related works have been performed using blast exposure of total animal bodies.[3,7,19,26–36] We have learned from reviewing these studies as well as from our own studies that issues of scaling remain a challenge. The blast energy imparted on an animal must be consistently scalable to the blast energy experienced by a service member in the field. Anatomic differences between models are also significant and must be accounted for. In turn, this arena of research would be much advanced if it were easier to obtain actual data on blast exposures along with their pathologic correlates in humans. However, the need for operational security poses a challenge regarding obtaining such data. In the mean time, we recommend collaborating with military medical and explosives experts to ensure that models are appropriate for the questions being addressed.

Our data demonstrate that rat mortality is remarkably higher when the unprotected rat body is exposed to blast, compared with head-directed or body-protected blast impacts of similar magnitude (Table 1). All rats but one subjected to head-directed unprotected body blast survived without visible behavioral signs of abnormality. Generally, these observations are in line with previous extensive studies by Stuhmiller et al. and Stuhmiller performed in rat and sheep.[3,20,37] A significantly lower threshold magnitude of blast that results in immediate rat lethality on exposure of unprotected rats versus head-directed, body-armored impact suggests the importance of systemic reactions that we would like to term "blastogenic

shock." Head-directed strong blast impacts resulted in severe morphologic brain damage including massive and focal hemorrhages (Fig. 3A) but did not lead to significant rat mortality. Moreover, these rats recovered rapidly from the blast exposure and anesthesia and did not show visible signs of behavioral abnormality within 24 hours to 14 days postblast (data not shown). Silver staining, that is, indicative of neurodegeneration,[38] was prominent in various regions of the brain, predominantly in deep areas of the rostral and caudal mesencephalon and diencephalon but not in the cortex (Fig. 3, B). This may suggest that the energy of the blast impulse is transmitted through the skull, induces head acceleration and jolting, and activates responses in deeper structures of the brain, mediated by the cerebral liquid and cisternae system, thus preventing significant injury to the cortex.

In previous studies, using mechanical impact controlled cortical impact (CCI) model of TBI in rats, we have convincingly demonstrated the important role for caspase-3–mediated apoptotic pathways in neuronal injury as well as the calpain-mediated oncosis/necrosis mechanisms.[39–41] We and others found that the signature cleavage products of aII-spectrin spectrin breakdown products (SBDPs) by caspases/calpain accumulated in brain tissue at sites of injury and CSF after brain injury in rats[42–44] and in human CSF after TBI.[17,41] Whether this mechanism operates after blast impact and what are its specific characteristics remain to be investigated.

In a recent study, rats were exposed to a direct single shock wave shot after craniotomy. The high-OP (>10 MPa) shock wave exposure resulted in hemorrhage and a significant increase in terminal deoxynucleotidyl transferase dUTP nick end labeling (TUNEL)-positive neurons with the maximum increase seen at 24 hours after the shock wave application.[45] Low-OP (1 MPa) shock wave exposure resulted in spindle-shaped changes in neurons and elongation of nuclei without marked neuronal injury. The administration of caspase-3 antagonist (Z-VAD-FMK) significantly reduced the number of TUNEL-positive cells observed 24 hours after high-OP shock wave exposure. The authors speculated that the threshold for shock wave-induced brain injury is under 1 MPa, a level that is lower than the threshold for other organs including lungs.[45] However, the model of blast injury used in this study is very similar to CCI model, which our group has been using for a number of years in rat TBI studies. The morphologic pattern of brain tissue injury in that model closely resembled the damage observed after CCI.[45]

A significant hippocampal accumulation of GFAP, and CNPase, established markers of activated glia, has been detected after blast (Figs. 4, B and 5, B). GFAP has only recently gained attention as a TBI biomarker when GFAP blood level was shown to be a good predictor of patient's mortality with sensitivity between 70% and 84% depending on the time it was measured after injury.[46,47] The roles for glia activation and GFAP as astrocyte marker after CCI in rats have been frequently reported.[48,49] However, GFAP levels in blood and CSF during experimental TBI have not been studied and its biomarker utility has not been validated, particularly in BBI models. Our data clearly demonstrate a rapid increase in serum GFAP within 24 hours after blast followed by a decline thereafter with a gradual accumulation in CSF (Fig. 6).

Similar to GFAP, NSE was substantially increased in serum at 24 hours and 48 hours after blast, whereas the CSF NSE concentrations showed a tendency to increase, but it was not statistically significant (Fig. 7). NSE initially held promise as a brain injury biomarker because it was originally thought to be strictly neuronal.[23] The sensitivity and specificity of serum NSE after pediatric TBI determined by receiver operating characteristic curves were found to be 71% and 64%, respectively.[14] After multiple trauma, elevated NSE levels have been observed but systemic NSE increased by similar degrees, with and without TBI, limiting its ability to discriminate brain injury magnitude.[50] In addition, NSE has a long half-life, >20 hours in serum that may account for its limitation as a TBI biomarker.[51]

UCH-L1 has attracted attention as a crucial enzyme linked to Parkinson's disease and memory and is selectively expressed in neurons at high levels.[52–55] Experimental evidence suggests that UCH-L1 plays a critical role in removal of excessive, oxidized, or misfolded proteins both during normal and neuropathological conditions. The release of UCH-L1 has been shown in lumbar CSF samples from 19 surgical cases of aortic aneurysm repair and 7 involving cardiopulmonary bypass with deep hypothermic circulatory arrest.[53] Recently, it has been shown by our group that the UCH-L1 is a potential biomarker for TBI in CCI models in rats.[56] We developed, validated, and used SW ELISA assay for quantitative detection of UCH-L1 in biofluids including plasma/serum with a high sensitivity of the assay of 10 pg/mL. Using the UCH-L1 SW ELISA, we showed a strong correlation between UCH-L1 levels in human CSF and outcome after severe TBI in patients.[57] Here, in an experimental study, we demonstrate a rapid and significant release and accumulation of UCH-L1 in blood at 24 hours after blast exposure compared with naïve and shams animal followed by a gradual decline (Fig. 8). The CSF levels of UCH-L1, although not statistically significant, were slightly elevated and persistent for a longer period of time after blast (Fig. 8, A). These data suggest an increase of extensity of neuronal ubiquitination that may contribute to neurodegeneration as long consequences of blast exposure.

Taken together, a characteristic time course of GFAP, NSE, and UCH-L1 indicates a blood-brain barrier disruption after severe blast exposure triggering the pathologic events in the brain that lead to hemorrhages, gliosis, and glia/neuronal interactions and may lead to neuronal degeneration.

In summary, we developed a comprehensive and reproducible model of blast exposure and injury in rats. The data suggest that mechanisms underlying blast brain injuries, particularly mild and moderate, appear to be distinct from those imposed by mechanical impact and may be triggered by systemic, cerebrovascular, and neuroglia responses as consecutive but overlapping events.

ACKNOWLEDGMENTS

We thank Dr. Zhiqun Zhang, Ms. Qiushi Tang, Ms. Olena Glushakova, and Ms. Olga Tchigrinova for their ex-

cellent technical assistance and Mr. Archie Svetlov for his help in preparation of the manuscript for publication.

REFERENCES

1. Cramer F, Paster S, Stephenson C. Cerebral injuries due to explosion waves, cerebral blast concussion; a pathologic, clinical and electroencephalographic study. *Arch Neurol Psychiatry.* 1949;61:1–20.
2. Murthy JM, Chopra JS, Gulati DR. Subdural hematoma in an adult following a blast injury. Case report. *J Neurosurg.* 1979;50:260–261.
3. Stuhmiller JH, Ho KH, Vander Vorst MJ, Dodd KT, Fitzpatrick T, Mayorga M. A model of blast overpressure injury to the lung. *J Biomech.* 1996;29:227–234.
4. Savic J, Tatic V, Ignjatovic D, et al. [Pathophysiologic reactions in sheep to blast waves from detonation of aerosol explosives]. *Vojnosanit Pregl.* 1991;48:499–506 [in Serbian].
5. Jaffin JH, McKinney L, Kinney RC, et al. A laboratory model for studying blast overpressure injury. *J Trauma.* 1987;27:349–356.
6. Guy RJ, Kirkman E, Watkins PE, Cooper GJ. Physiologic responses to primary blast. *J Trauma.* 1998;45:983–987.
7. Cernak I, Wang Z, Jiang J, Bian X, Savic J. Cognitive deficits following blast injury-induced neurotrauma: possible involvement of nitric oxide. *Brain Inj.* 2001;15:593–612.
8. Chavko M, Adeeb S, Ahlers ST, McCarron RM. Attenuation of pulmonary inflammation after exposure to blast overpressure by N-acetylcysteine amide. *Shock.* 2009;32:325–331.
9. Saljo A, Bao F, Haglid KG, Hansson HA. Blast exposure causes redistribution of phosphorylated neurofilament subunits in neurons of the adult rat brain. *J Neurotrauma.* 2000;17:719–726.
10. Svetlov SI, Larner SF, Kirk DR, Atkinson J, Hayes RL, Wang KK. Biomarkers of blast-induced neurotrauma: profiling molecular and cellular mechanisms of blast brain injury. *J Neurotrauma.* 2009;26:913–921.
11. Bazarian JJ, Zemlan FP, Mookerjee S, Stigbrand T. Serum S-100B and cleaved-tau are poor predictors of long-term outcome after mild traumatic brain injury. *Brain Inj.* 2006;20:759–765.
12. Piazza O, Storti MP, Cotena S, et al. S100B is not a reliable prognostic index in paediatric TBI. *Pediatr Neurosurg.* 2007;43:258–264.
13. Berger RP, Beers SR, Richichi R, Wiesman D, Adelson PD. Serum biomarker concentrations and outcome after pediatric traumatic brain injury. *J Neurotrauma.* 2007;24:1793–1801.
14. Berger RP, Adelson PD, Pierce MC, Dulani T, Cassidy LD, Kochanek PM. Serum neuron-specific enolase, S100B, and myelin basic protein concentrations after inflicted and noninflicted traumatic brain injury in children. *J Neurosurg.* 2005;103:61–68.
15. de Olmos JS, Beltramino CA, de Olmos de Lorenzo S. Use of an amino-cupric-silver technique for the detection of early and semiacute neuronal degeneration caused by neurotoxicants, hypoxia, and physical trauma. *Neurotoxicol Teratol.* 1994;16:545–561.
16. Switzer RC III. Application of silver degeneration stains for neurotoxicity testing. *Toxicol Pathol.* 2000;28:70–83.
17. Ringger NC, O'Steen BE, Brabham JG, et al. A novel marker for traumatic brain injury: CSF alpha II-spectrin breakdown product levels. *J Neurotrauma.* 2004;21:1443–1456.
18. Cooper PW. *Explosives Engineering.* New York, NY: Wiley-VCH; 1996.
19. Elsayed NM. Toxicology of blast overpressure. *Toxicology.* 1997;121:1–15.
20. Stuhmiller JH. Biological response to blast overpressure: a summary of modeling. *Toxicology.* 1997;121:91–103.
21. Doran JF, Jackson P, Kynoch PA, Thompson RJ. Isolation of PGP 9.5, a new human neurone-specific protein detected by high-resolution two-dimensional electrophoresis. *J Neurochem.* 1983;40:1542–1547.
22. Chiaretti A, Barone G, Riccardi R, et al. NGF, DCX, and NSE upregulation correlates with severity and outcome of head trauma in children. *Neurology.* 2009;72:609–616.
23. Vinores SA, Herman MM, Rubinstein LJ, Marangos PJ. Electron microscopic localization of neuron-specific enolase in rat and mouse brain. *J Histochem Cytochem.* 1984;32:1295–1302.
24. Taber KH, Warden DL, Hurley RA. Blast-related traumatic brain injury: what is known? *J Neuropsychiatry Clin Neurosci.* 2006;18:141–145.
25. Kirk DR, Faure JM, Gutierrez M, et al. Generation and analysis of blast waves from a compressed air-driven shock tube. *J Appl Mech.* In press.
26. Mayorga MA. The pathology of primary blast overpressure injury. *Toxicology.* 1997;121:17–28.
27. Cernak I, Radosevic P, Malicevic Z, Savic J. Experimental magnesium depletion in adult rabbits caused by blast overpressure. *Magnes Res.* 1995;8:249–259.
28. Cernak I, Savic VJ, Lazarov A, Joksimovic M, Markovic S. Neuroendocrine responses following graded traumatic brain injury in male adults. *Brain Inj.* 1999;13:1005–1015.
29. Elsayed NM, Gorbunov NV. Interplay between high energy impulse noise (blast) and antioxidants in the lung. *Toxicology.* 2003;189:63–74.
30. Gorbunov NV, Elsayed NM, Kisin ER, Kozlov AV, Kagan VE. Air blast-induced pulmonary oxidative stress: interplay among hemoglobin, antioxidants, and lipid peroxidation. *Am J Physiol.* 1997;272:L320–L334.
31. Chavko M, Prusaczyk WK, McCarron RM. Lung injury and recovery after exposure to blast overpressure. *J Trauma.* 2006;61:933–942.
32. Elsayed NM, Gorbunov NV. Pulmonary biochemical and histological alterations after repeated low-level blast overpressure exposures. *Toxicol Sci.* 2007;95:289–296.
33. Elsayed NM, Gorbunov NV, Kagan VE. A proposed biochemical mechanism involving hemoglobin for blast overpressure-induced injury. *Toxicology.* 1997;121:81–90.
34. Januszkiewicz AJ, Mundie TG, Dodd KT. Maximal exercise performance-impairing effects of simulated blast overpressure in sheep. *Toxicology.* 1997;121:51–63.
35. Cernak I, Ignjatovic D, Andelic G, Savic J. [Metabolic changes as part of the general response of the body to the effect of blast waves]. *Vojnosanit Pregl.* 1991;48:515–522 [in Serbian].
36. Cernak I, Savic J, Mrsulja B, Duricic B. [Pathogenesis of pulmonary edema caused by blast waves]. *Vojnosanit Pregl.* 1991;48:507–514 [in Serbian].
37. Stuhmiller JH. *Blast Injury Thresholds. JAYCOR Technical Report on Contract DAMD17–89-C-9150*. San Diego: Department of the Army; 1990.
38. Tenkova TI, Goldberg MP. A modified silver technique (de Olmos stain) for assessment of neuronal and axonal degeneration. *Methods Mol Biol.* 2007;399:31–39.
39. Wang KK, Ottens AK, Liu MC, et al. Proteomic identification of biomarkers of traumatic brain injury. *Expert Rev Proteomics.* 2005;2:603–614.
40. Ottens AK, Kobeissy FH, Golden EC, et al. Neuroproteomics in neurotrauma. *Mass Spectrom Rev.* 2006;25:380–408.
41. Pineda JA, Wang KK, Hayes RL. Biomarkers of proteolytic damage following traumatic brain injury. *Brain Pathol.* 2004;14:202–209.
42. Pike BR, Flint J, Dutta S, Johnson E, Wang KK, Hayes RL. Accumulation of non-erythroid alpha II-spectrin and calpain-cleaved alpha II-spectrin breakdown products in cerebrospinal fluid after traumatic brain injury in rats. *J Neurochem.* 2001;78:1297–1306.
43. Pike BR, Zhao X, Newcomb JK, Posmantur RM, Wang KK, Hayes RL. Regional calpain and caspase-3 proteolysis of alpha-spectrin after traumatic brain injury. *Neuroreport.* 1998;9:2437–2442.
44. Beer R, Franz G, Srinivasan A, et al. Temporal profile and cell subtype distribution of activated caspase-3 following experimental traumatic brain injury. *J Neurochem.* 2000;75:1264–1273.
45. Kato K, Fujimura M, Nakagawa A, et al. Pressure-dependent effect of shock waves on rat brain: induction of neuronal apoptosis mediated by a caspase-dependent pathway. *J Neurosurg.* 2007;106:667–676.
46. Nylen K, Ost M, Csajbok LZ, et al. Increased serum-GFAP in patients with severe traumatic brain injury is related to outcome. *J Neurol Sci.* 2006;240:85–91.
47. Pelinka LE, Kroepfl A, Leixnering M, et al. GFAP versus S100B in serum after traumatic brain injury: relationship to brain damage and outcome. *J Neurotrauma.* 2004;21:1553–1561.
48. Urrea C, Castellanos DA, Sagen J, Tsoulfas P, Bramlett HM, Dietrich WD. Widespread cellular proliferation and focal neurogenesis after

traumatic brain injury in the rat. *Restor Neurol Neurosci*. 2007;25: 65–76.
49. Johnson EA, Svetlov SI, Pike BR, et al. Cell-specific upregulation of survivin after experimental traumatic brain injury in rats. *J Neurotrauma.* 2004;21:1183–1195.
50. Pelinka LE, Hertz H, Mauritz W, et al. Nonspecific increase of systemic neuron-specific enolase after trauma: clinical and experimental findings. *Shock.* 2005;24:119–123.
51. Ingebrigtsen T, Romner B. Biochemical serum markers for brain damage: a short review with emphasis on clinical utility in mild head injury. *Restor Neurol Neurosci.* 2003;21:171–176.
52. Liu Z, Meray RK, Grammatopoulos TN, et al. Membrane-associated farnesylated UCH-L1 promotes {alpha}-synuclein neurotoxicity and is a therapeutic target for Parkinson's disease. *Proc Natl Acad Sci U S A.* 2009;106:4635–4640.
53. Siman R, Roberts VL, McNeil E, et al. Biomarker evidence for mild central nervous system injury after surgically-induced circulation arrest. *Brain Res.* 2008;1213:1–11.
54. Harada T, Harada C, Wang YL, et al. Role of ubiquitin carboxy terminal hydrolase-L1 in neural cell apoptosis induced by ischemic retinal injury in vivo. *Am J Pathol.* 2004;164:59–64.
55. Osaka H, Wang YL, Takada K, et al. Ubiquitin carboxy-terminal hydrolase L1 binds to and stabilizes monoubiquitin in neuron. *Hum Mol Genet.* 2003;12:1945–1958.
56. Kobeissy FH, Ottens AK, Zhang Z, et al. Novel differential neuroproteomics analysis of traumatic brain injury in rats. *Mol Cell Proteomics.* 2006;5:1887–1898.
57. Papa L, Akinyi L, Liu MC, et al. Ubiquitin C-terminal hydrolase is a novel biomarker in humans for severe traumatic brain injury. *Crit Care Med*. 2010;38:138–144.

Abstract presented at Advanced Technology Applications for Combat Casualty Care (ATACCC) 2009
St. Pete Beach, August 16-19, 2009

Molecular and Cellular Fingerprints of Brain Overpressure Load: Potential Biomarkers of Blast Brain Injury

V. I. Prima[1], D. R. Kirk[2] , H. M. Gutierrez[2], M. V. Pereira[2], K. C. Curley[3], R. L. Hayes[1], K. W. Wang[1], S. I. Svetlov[1]

[1]Banyan Biomarkers, Inc., Alachua, FL; [2]Florida Institute of Technology, Melbourne, FL ; [3]U.S. Army Medical Research and Materiel Command (MRMC), Fort Detrick, MD

A comprehensive experimental model for studies of controlled blast wave impact in rats is presented. Repeatable blast signatures of controlled duration, peak pressure and transmitted impulse enable to reproduce blast impact in laboratory animals in accurate fashion. Animal survival, brain pathomorphology and the levels of putative biomarkers of brain injury GFAP, NSE and UCH-L1 was examined in CSF and blood after head-directed non-penetrating blast of 358 kPa magnitude at surface for 10 msec. The high speed imaging demonstrated strong head acceleration/jolting accompanied by typical intracranial hematomas and brain swelling. The microscopic injury was revealed by prominent silver staining in the deep brain areas including nucleus subthalamicus zone suggesting both diffused and focal neurodegeneration. GFAP and CNPase, markers of astroglia and oligodendroglia, accumulated substantially in hippocampus and, to a lesser extent, in the cortex 24 h after blast and persisted for 30 days post-blast. In blood however, GFAP content significantly increased 24 h after injury, followed by a decline thereafter and subsequent accumulation in CSF in a time-dependent fashion. A similar profile is shown for neuronal marker UCH-L1 increase in blood, while increased CSF levels of UCH-L1 persisted throughout 14 days after blast exposure and varied significantly in individual rats. NSE levels in blood were significantly elevated within 24 and 48 hours post-blast. The proposed model of controlled non-penetrating blast in rats, demonstrates the critical pathological and biochemical signatures of blast brain injury that may be triggered by cerebrovascular responses, including blood brain barrier disruption, glia responses and neuro-glial alterations.

MILITARY HEALTH RESEARCH FORUM

PROCEEDINGS

August 31 - September 3, 2009

Kansas City, MO

Military Health Research Forum 2009 Biomarkers I **COMPREHENSIVE EXPERIMENTAL MODELS FOR PROFILING MECHANISMS AND DEVELOPING BIOMARKERS OF BLAST BRAIN INJURY**

Stanislav Svetlov
Banyan Biomarkers, Inc.

There is a lack of pertinent reproducible models within the blast injury framework, including generators that precisely control parameters of the blast wave. This makes it difficult to predict the degree of impact, which depends on characteristics of the blast wave affecting the body, for development of diagnostics and mitigation. A comprehensive experimental model of blast exposure has been developed and implemented including construction of a compact vertical shock tube. Initial experiments were performed by placing animals on-axis of the shock tube and applying blast of various magnitude and duration that included exposure to gas venting. Total body blast exposure had a much greater impact on mortality compared to head-directed exposure of a similar magnitude. The high-speed imaging reflected strong head acceleration upon head-directed blast, and brain pathomorphology showed intracranial hematomas and brain swelling. This severe damage was accompanied by strong positive silver staining in the several deep brain areas indicating both diffused and focal neurodegeneration. The severe brain injury was a result of combined blast wave exposure (peak overpressure) and gas venting, which is an artifact inherent to shock tube operation, is not associated with the actual blast events and is difficult to control. A solution has been employed to address this problem: Placing the animal at an off-axis angle avoids venting and allows producing and controlling mild blast wave exposures. There was no detectible breakdown of αII-spectrin in the rat cortex after severe direct blast exposure, in contrast to an extensive αII-spectrin proteolytic cleavage seen after mechanical controlled cortical impact. GFAP accumulated in the cortex starting at 24 h after blast exposure and reached maximum levels at 14 days post-blast. However, GFAP content significantly increased in blood 24 h after injury, followed by a decline thereafter and accumulation in CSF in a time-dependent fashion. A similar profile is shown for UCH-L1 increase in blood, while increased CSF levels of UCH-L1 persisted throughout 14 days after blast exposure and varied significantly in individual rats. NSE levels in blood were significantly elevated within 24 and 48 hours post-blast. In summary, we developed a comprehensive model of blast exposure and injury in rats. Our data suggests that mechanisms underlying blast brain injuries, particularly mild and moderate, may be distinct from those imposed by mechanical impact and may be triggered by systemic, cerebrovascular, and neuroglia responses as consecutive but overlapping events.

This work was supported by the U.S. Army Medical Research and Materiel Command under W81XWH-08-1-0376.

Abstracts
from

The Second Joint Symposium of The National and International Neurotrauma Societies

September 7–11, 2009
Santa Barbara, CA

P291

MORPHOLOGICAL AND BIOCHEMICAL SIGNATURES OF BRAIN INJURY FOLLOWING HEAD-DIRECTED CONTROLLED BLAST OVER-PRESSURE IMPACT

Stanislav Svetlov[1], Victor Prima[1], Daniel Kirk[2], Joseph Atkinson[2], Hector Gutierrez[2], Kenneth Curley[3], Ronald Hayes[1], Kevin Wang[1]
[1]*Banyan Biomarkers, Inc, Alachua, United States,* [2]*Florida Institute of Technology, Melbourne, United States,* [3]*U.S. Army Medical Research and Material Command, Fort Detrick, MD, United States*

A comprehensive experimental model for studies of controlled blast wave impact in rats is presented. Repeatable blast signatures of controlled duration, peak pressure and transmitted impulse enable to reproduce blast impact in laboratory animals in accurate fashion.

Animal survival, brain pathomorphology and the levels of putative biomarkers of brain injury GFAP, NSE and UCH-L1 was examined in CSF and blood after head-directed non-penetrating blast of 358 kPa magnitude at surface for ~10 msec. The high speed imaging demonstrated strong head acceleration/jolting accompanied by typical intracranial hematomas and brain swelling. The microscopic injury was revealed by prominent silver staining in the deep brain areas including nucleus subthalamicus zone suggesting both diffused and focal neurodegeneration. GFAP and CNPase, markers of astroglia and oligodendroglia, accumulated substantially in hippocampus and, to a lesser extent, in the cortex 24 h after blast and persisted for 30 days post-blast. In blood however, GFAP content significantly increased 24 h after injury, followed by a decline thereafter and subsequent accumulation in CSF in a time-dependent fashion. A similar profile is shown for neuronal marker UCH-L1 increase in blood, while increased CSF levels of UCH-L1 persisted throughout 14 days after blast exposure and varied significantly in individual rats. NSE levels in blood were significantly elevated within 24 and 48 hours post-blast.

The proposed model of controlled non-penetrating blast in rats, demonstrates the critical pathological and biochemical signatures of blast brain injury that may be triggered by cerebrovascular responses, including blood brain barrier disruption, glia responses and neuro-glial alterations.

P292

DEVELOPMENT OF POST-TRAUMATIC EPILEPSY IN C57BL/6 MICE AFTER CONTROLLED CORTICAL IMPACT INJURY

Tamuna Bolkvadze, Nissinen Jari, Kharatishvili Irina, Pitkänen Asla
Department of Neurobiology, University of Kuopio, Kuopio, Finland

Objective: Traumatic brain injury (TBI) is estimated to cause 10–20% of symptomatic epilepsies. The genetic risk factors and molecular mechanisms leading to post-traumatic epilepsy (PTE) are unknown. The present study investigated whether controlled cortical impact (CCI) -induced TBI triggers epileptogenesis in C57BL/6 mice that is the most widely used genetic background to produce genetically modified mice.
Materials and Method: CCI brain injury was induced in 8–10 wk old male C57BL/6JOlaHsd mice (Harlan, Netherlands) (22–26g) to parietal cortex over left hippocampus (14 shams, 50 CCI). Injury velocity was 5 m/s and depth 0.5 mm. Four months after CCI, cortical electrodes were inserted into the skull. The first continuous video-EEG recording to detect the occurrence of spontaneous seizures was performed at 6 months post-CCI. After the first 2-wk of monitoring, pentyleneterazol (PTZ, 50 mg/kg, i.p.) seizure threshold test was performed under video-EEG to detect lowered seizure threshold (latency to the first seizure, number of epileptiform discharges (ED), total number of spikes within 1 h after PTZ). Thereafter, monitoring was continued for another 2 wk. The second video-EEG monitoring of 2-wk was conducted at 9 months post-TBI.
Results: At 6 months post-injury, 4 of 43 mice had secondarily generalized spontaneous seizures. Epileptiform spiking activity was detected in about 80% of injured mice. PTZ test indicated reduced latency to the first spike ($p < 0.01$) and increased total number of spikes ($p < 0.01$) in injured mice as compared to controls. The second video-EEG monitoring at 9 months post-injury did not reveal any new mice with spontaneous seizures.
Conclusion: CCI –induced TBI leads to the development of lowered seizure threshold and even the occurrence of spontaneous seizures in C57BL/6 mice.
This study was supported by the CURE, the Academy of Finalnd, and the Sigrid Juselis Foundation.

P293

TIME LAPSE EXPERIMENTS SHOW NO INCREASE IN CELL DEATH AFTER PHYSICAL INJURY ALONE IN A CELL CULTURE MODEL OF TBI

Camilla Lööv, Lars Hillered, Anna Erlandsson
Section of Neurosurgery, Department of Neuroscience, Uppsala University, Uppsala, Sweden

The molecular and cellular mechanisms involved in neuronal cell death following traumatic brain injury (TBI) are still poorly understood. To be able to follow the series of events affecting specific neurons in the acute phase of the injury we have set up an *in vitro* model of TBI based on physical damage by controlled cutting to a mixed culture of cortical neurons and glia in culture. This method enables studies with time lapse microscopy and is therefore suitable for detailed investigations of neuronal responses to injury, including cell death, cell-cell interactions and axonal regeneration. Basically, E14 mouse cortical stem cells are expanded as neurospheres and plated on laminin coated glass cover slips. After 8–10 days in serum-free medium without mitogens the cells have differentiated into neurons (ß III tubulin+), astrocytes (GFAP+) and oligodendrocytes (O4+).The injury is induced by controlled cutting with a razor-blade through the cells (10 linear cuts with a 3 mm distance) in both directions. Surprisingly, our time lapse experiments demonstrate that mechanical injury to neurons and glial cells in culture does not induce cell death. A high cellular activity was observed in the injured cultures including cell migration and axonal regrowth. The time lapse data was further supported by TUNEL and Fluoro-Jade stainings, demonstrating no difference in the number of apoptotic and necrotic cells in injured cultures compared to control cultures. Furthermore the neurons around the scratch were shown to express the growth cone marker GAP43 indicating regeneration of neurites. However, addition of the reactive oxygen species hydrogen peroxide to the cell cultures immediately after injury show that injured neurons are much more sensitive to oxidative stress than uninjured controls. Our data suggest that physical injury by itself does not cause neuronal death in this cell culture model of TBI, and that neurons have a tremendous survival capacity if not exposed to harmful substances in addition to the injury. Next we will investigate the effect of various combinations of growth factors on neuronal survival after physical injury in combination with hydrogen peroxide treatment.

P294

AGE-DEPENDENT CHANGES IN GENE EXPRESSION FOLLOWING COMPLETE SPINAL CORD TRANSECTION IN NEONATAL OPOSSUMS (*MONODELPHIS DOMESTICA*)

Norman Saunders[1], Jessie Truettner[2], C. Joakim Ek[1], Katarzyna Dziegielewska[1], Ben Wheaton[1], W. Dalton Dietrich[2]
[1]*University of Melbourne, Parkville, Victoria, 3010, Australia,* [2]*University of Miami, Miami, FL, United States*

Severe spinal cord injury results in a loss of a variety of motor, sensory, and autonomic functions. Previously, it has been reported that in neonatal opossums, regeneration of severed axons and functional recovery can occur following spinal cord injury (SCI), but that this ability to recover decreases with age. The South American opossum, *Monodelphis domestica*, makes an ideal model for examining the effects of SCI during early development, as the young are very immature at birth. Very young animals are able to regenerate 50% of injured axons and develop substantially normal function (Fry et al., J. Comp Neurol., 466, 422–444, 2003) whereas animals 3–4 weeks older do not (see Wheaton et al. this meeting). This study uses quantitative RT-PCR to analyze the differences in gene expression of key inflammatory, growth factor and adhesion molecule genes in the injured spinal cord of P7 versus P28 animals at three times after injury: 3 h, 24 h, and 7 days. In injured spinal cord specimens, major cytokines and their receptors all went up sharply in P7 animals and stayed elevated up to 7 days after injury, for example: IL-1β: 38 fold $p < 0.005$, TNF-α: 4.3 fold $p < 0.005$, IL-6: 8.6 fold $p < 0.01$, IL1r1 and TNFr1a both 5 fold higher, and stayed elevated up to 7 days after injury. In P28 animals, in general, the increases were less pronounced, but also persisted for 7 days. Growth factors did not increase to the same extent as seen with the cytokines. NGF and NT3 and their receptors TRK-1 and TRK-3 showed minimal or no increases at the early time point (1–2 fold increases at 3 h). TGF-β was increased in both P7 and P28 at 3–24 h (1–2 fold, $p < 0.05$). Adhesion/guidance molecules N-CAM, Eph4A, and TPA showed no significant increases at either age with the exception of P28 3 h animals (N-CAM: 2.4 fold $p < 0.005$ and TPA: 1.9 fold $p < 0.05$). These changes reflect some of the changes that are occurring at and rostral to the injury site. Changes in expression of these and other genes in the brain stem of injured animals may show very different patterns of expression in the regenerating animals versus the non-regenerating animals. Understanding patterns of gene expression responses following SCI may allow for the development of novel treatments to protect and promote recovery after injury.

Supported by Victorian Neurotrauma Initiative, Shriners Hospitals & The Miami Project to Cure Paralysis.